TERAHERTZ TIME OF FLIGHT DETECTION FOR ABSOLUTE THICKNESS MEASUREMENT OF SINGLE SIDE POLISHED SILICON WAFERS

by

Javaid Ikram

A thesis submitted to the faculty of
The University of North Carolina at Charlotte
in partial fulfillment of the requirements
for the degree of Master of Science in
Optical Science and Engineering

Charlotte

2010

Approved by

_____
Dr. Angela D. Davies

_____
Dr. Faramarz Farahi

_____
Dr. Tsing-Hua Her

_____
Dr. Robert Hocken

ABSTRACT

JAVAID IKRAM. Terahertz time of flight detection for absolute thickness measurements of single sided silicon wafers. (Under the direction of DR. ANGELA D. DAVIES)

We present a solution for a major challenge in semiconductor manufacturing, which is the measurement of the absolute thickness of single side polished silicon wafers. Our thesis is that terahertz time of flight detection can be used in other non-destructive measurement applications in precision engineering. In particular, we propose that this method can be used to measure the thickness of single-sided silicon wafers. A transmission mode terahertz time of flight system was designed, constructed and used to demonstrate this technique. A measurement capability and correlation analysis of our system was performed by characterizing the thickness of lightly doped silicon wafers. This is a challenging measurement in a manufacturing environment and a terahertz approach represents a significant advance. Furthermore, the absolute thickness measurement and refractive index estimate of an unknown material was performed. The results show that the terahertz time of flight metrology system is repeatable and has a measurement speed of less then 2 minutes making it suitable for high volume process control.

DEDICATION

To my parents, the source of endless love and support.

ACKNOWLEDGEMENTS

I would like to thank my advisor Dr. Angela Davies who directed this project with vision, elegance and patience. Without her guidance and support I would never have been able to complete this project. I would like to thank Dr. Faramarz Farahi and Dr. Robert Hocken for guiding me at critical stages of the project with brilliant ideas and solutions. I would also like to express my sincere gratitude to Dr. Tsing-Hua Her for helping me with the femtosecond laser alignment and operation. I would like to thank the entire Physics and Optical Science department at UNC Charlotte for their support.

I would like to thank Dr. Xi-Cheng Zhang and his associates at Rensselaer Polytechnic Institute for helping us with technical advice and assistance.

Funding for this project was provided by the industrial affiliates of the center for precision metrology at the University of North Carolina at Charlotte.

I would like to thank my committee members for the time and effort they spent in reviewing this manuscript and help make it a better one.

TABLE OF CONTENTS

CHAPTER 1: INTRODUCTION

1. 1 Project history and motivation

Terahertz radiation refers to far infrared or sub millimeter radiation and its frequency lies between the microwave and infra red region of the electromagnetic spectrum. In terms of wavelength, terahertz radiation corresponds to 10^{12} Hz and hence 0.3 mm in free space. The advent of ultrafast lasers heralded the start of the terahertz era. Technological advances and applied research in terahertz radiation has increased exponentially ever since.

The terahertz spectral region lies between the electronic part and the optics part of the electromagnetic spectrum and is referred to as the terahertz "gap". Photon energies in the terahertz region are below the electronic state transition energies in material that are necessary for optical sources. Moreover, terahertz photons cannot excite electrons above the band gap energy in a photodiode. On the other hand of the gap, terahertz frequencies are too high to be directly generated and detected by microwave technology. These technological challenges in generating and detecting terahertz radiation are overcome using ultrafast optics. Generation and detection is still difficult, consequently terahertz research was relatively unexplored until recently. Source and detector advances in the nineties initiated tremendous research growth, particularly in the areas of medical imaging and homeland security. The radiation is non-ionizing; with low scattering and

deep penetration into many insulating materials. And, many materials there are unique chemical signatures in the terahertz absorption and/or transmission spectra. Current research focus is in areas such as cancer screening, chemical and bio-agent detection, and concealed weapon detection [1-3].

1.2 Experimental plan

The overall project objective was to move in a direction with terahertz research and explore the potential for applications to non destructive testing and precision metrology. Applications in precision engineering and precision metrology are relatively unexplored. Terahertz radiation has potential for precision metrology of internal structures or defects in insulating materials such as coatings, ceramics, insulation and many composite materials that are difficult or impossible to characterize otherwise. Examples include paint film thickness, voids, crack, and internal geometries. UNC Charlotte and the CPM Affiliates program, with our knowledge of precision metrology, interferometry, and applications, have the unique expertise to develop this potential new branch of precision metrology.

The majority of terahertz research targets applications in medical imaging and homeland security. The Center for Terahertz Research at Rensselaer Polytechnic Institute (RPI) in New York is one of the leaders in this field [4]. A literature survey shows few applications in precision metrology. There is an industry-focused effort in Germany between the Fraunhofer IOF and the IAP of the Friedrich-Schiller-University, focusing on fabrication of terahertz optical components and sources and detector advances suitable for industry [5]. Also, a group at Osaka University in Japan published a paper November 2005 on terahertz measurements of paint thickness [6].

Our focus is on applications of terahertz metrology for precision engineering manufacturing. We leveraged our expertise in interferometry and optical test methods to develop measurement configurations and methods. Source and detector advances were outside the scope of this project. Instead we leveraged the tremendous amount of ongoing research at other institutions. We continuously monitored these advances to maintain an ongoing projection of ultimate measurement capabilities in our area.

Our thesis is that terahertz time of flight detection can be used in other non-destructive measurement applications in precision engineering applications. In particular, we propose the method can be used to measure the thickness of single-sided silicon wafers. This is a challenging measurement in a manufacturing environment and a terahertz approach represents a significant advance.

In this project a transmission mode terahertz time of flight system was designed, constructed and used to demonstrate the measurement of the absolute thickness of single side polished silicon wafers. We build our measurement capabilities in stages. Ongoing work with ultra-fast pulsed laser in the Physics and Optical Science Department was leveraged for this project. Our knowledge in interferometry, optical test methods, and uncertainty assessment was directly applicable to this work.

The rest of chapter 1 investigates different techniques in non destructive testing and compares them to terahertz time domain metrology to motivate our research. This technique and the related technology are described in detail in chapters 2 and 3. In chapter 2 we provide an overview of the source and detector technology with a focus on pulsed terahertz generation and detection methods. Chapter 3 details our experimental plan and describes the setup of our terahertz metrology system. Experimental procedures

are results are presented in chapter 4. We conclude with a summary of the major achievements. In the final chapter, Chapter 5, we suggest ideas for future work in order to upgrade the system and enhance the measurement capabilities.

1.3 Terahertz spectral region

The boundaries of the terahertz region are somewhat arbitrary and vary within the terahertz research community. This ambiguity is a result of different methods of generation and detection as well as application considerations. Commonly used standards define the terahertz region as the portion of the electromagnetic spectrum between 0.1 THz to 30 THz (see figure 1). As we can see from figure 1, the commonly used units and conversions are the following [7]:

- Frequency = 1 THz
- Angular frequency = 6.28 THz
- Period = 1 ps
- Wavelength = 300 um
- Wavenumber = 33.3 cm^{-1}
- Photon energy = 4.14 meV
- Temperature = 48K

As described earlier, this region has been difficult to operate in because of the lack of terahertz source and detector technology. A milestone in the development of terahertz science and technology came in the 1970s when Shen and co workers demonstrated the generation of terahertz radiation from a non linear electro optic crystal [8]. Ultrafast lasers and antenna technologies developed in the 1980s enhanced the progress of terahertz research. Chapter 2 is dedicated to terahertz source and detector

technologies. The biggest advantage of using terahertz radiation is its application in non destructive testing.

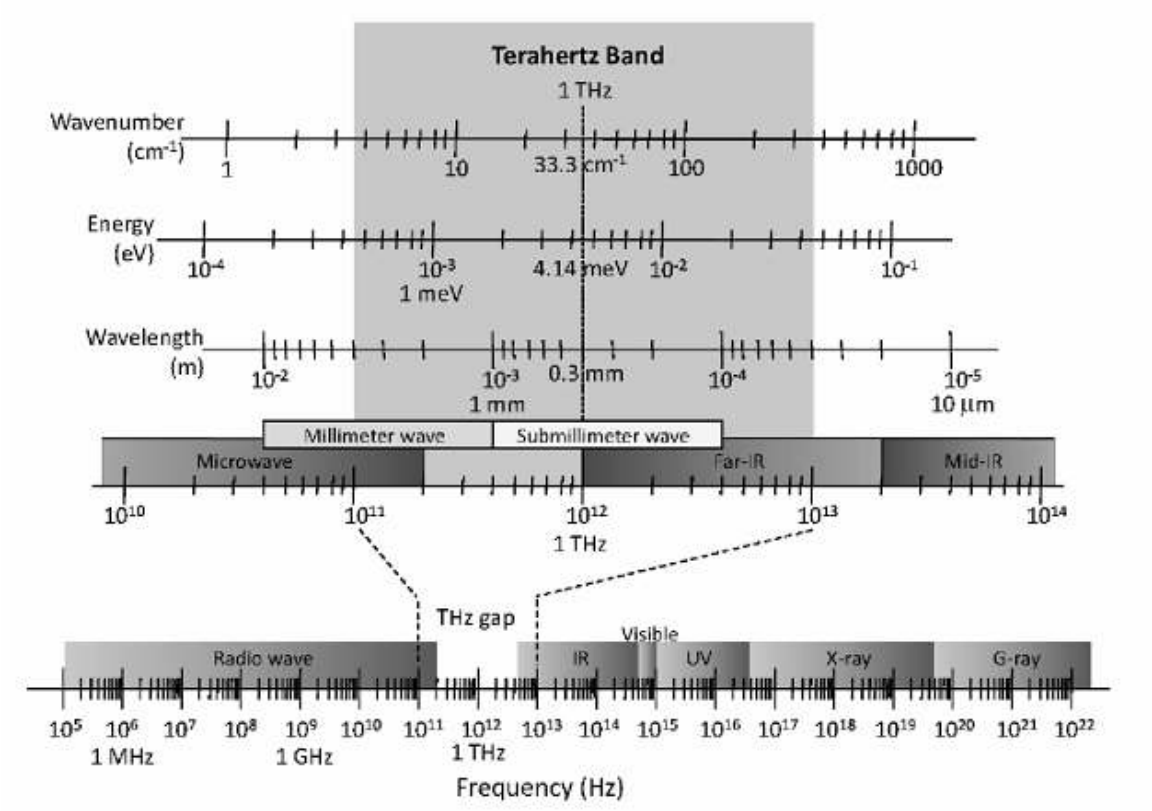

Figure 1: The terahertz gap in the electromagnetic spectrum [7]

1.4 Non destructive testing methods for thickness measurements

The American Society for Non Destructive Testing defines non destructive testing as the following:

"Non destructive evaluation is the examination of an object with technology that does not affect the object's future usefulness [9]". Non destructive testing may be used as a method to evaluate a finished product. As the definition implies, the finished part is not damaged and is useful for further use. Some techniques for non destructive testing are discussed in this section.

1.4.1 Eddy current

The Eddy current measurement technique can be used to measure conductive material. It is typically used to non-destructively test parts for aerospace and automotive industry. The method measures the material response to a magnetic field over a range in the electromagnetic spectrum. This range is usually a few kHz to several MHz. The probe is simply an AC transformer. Conductive materials are inspected through magnetic inductance. Figure 2 shows an Eddy current meter. The method only inspects conductive materials such as metals [10]. Conductivity variations can reveal a wide variety of information about a material. Cracks voids and thicknesses can be calculated using eddy current testing.

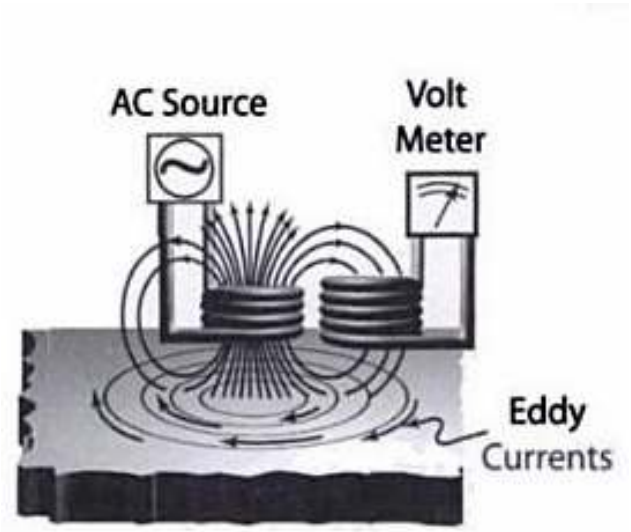

Figure 2: Eddy current measurement for non destructive testing [10].

1.4.2 Ultrasonic non destructive testing

Ultrasonic transducers are used for non destructive testing of solids, liquids and gases. Microstructures and material characteristics may be identified using this technique. Time domain transducers measure the time of flight to identify thickness and measure other properties of the object. Ultrasonic measurements can identify defects in the material during the manufacturing process. Different configurations are available for

ultrasonic probe measurements. Figure 3 illustrates the transmission mode measurement of medium using ultrasonic transducers.

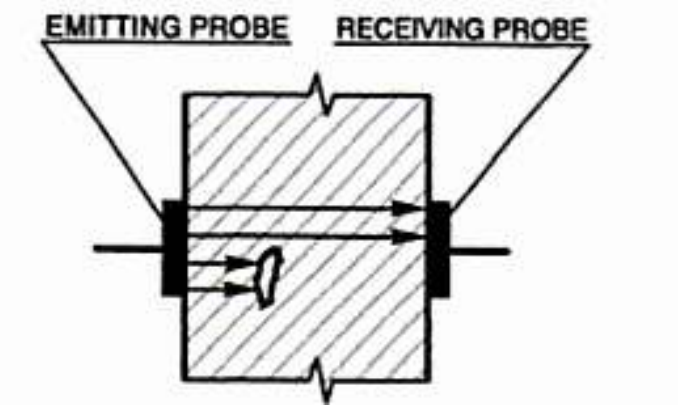

Figure 3: Transmission mode ultrasonic detection [11].

The ultrasonic wave transmits from the transmitter to the receiver through the measured medium [11]. A time of flight measurement is made between the free space propagation of the ultrasonic wave and compared to the time of flight measurement in the presence of the sample between the probes. This method enables measurement of thickness of the material.

1.4.3 Optical methods in non destructive testing

Optical methods in non destructive testing are among the most important because of their non contact nature. The main advantages of optical non destructive methods are the following:

- The measurements are non contact and don't require probes or surface contact.
- Real time measurements are possible using sensors such as Charged Coupled Devices (CCD) and photodiodes

- Often is a two or three dimensional measurement and the results are available over a field of view.

Precise knowledge of the material to be measured is often required since the measurements usually dependent on the refractive index in transmission-based measurement. Examples of optical-based non destructive test methods for thickness in particular, are given below.

1.4.3.1 Confocal microscopy

Confocal microscopy can be used to measure the thickness of transparent sheets using a process called optical splicing. The sensitivity or vertical resolution can be around 10 to 15 nm for lower magnification objectives [12]. The light reflected from different surfaces causes an axial response. The position of the peaks corresponds to the axial response and represents the interface of different medium. The amplitude of the peaks depends on the ratio of the refractive indices at the interfaces. Figure 4 illustrates the measurement technique.

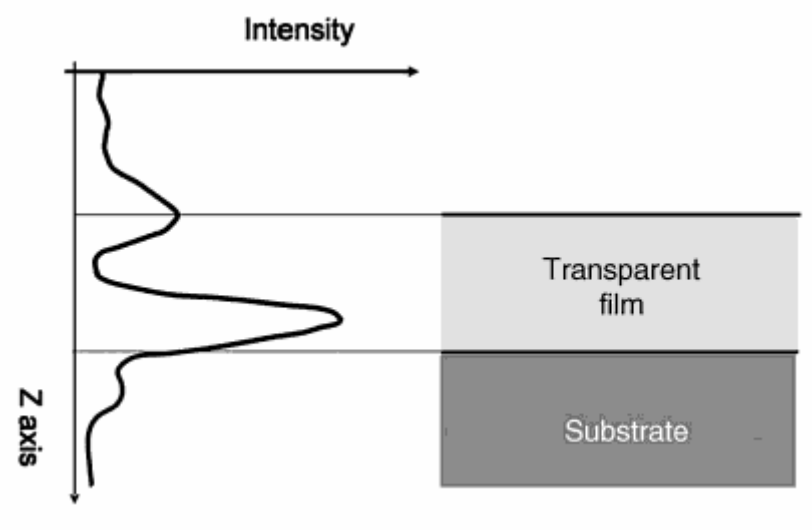

Figure 4: Confocal microscopy for measurement of film thickness [12].

The materials used in this technique need to be transparent to the wavelength of light used hence limiting their applications. This imposes a measurement limitation for some applications.

1.4.3.2 Infrared interferometry

The infrared region of the electromagnetic spectrum can be used to measure the thickness of materials opaque at visible frequencies. Figure 5 shows a practical interferometer in the Fizeau configuration implemented at the National Institute of Standards and Technology using infrared light [13].

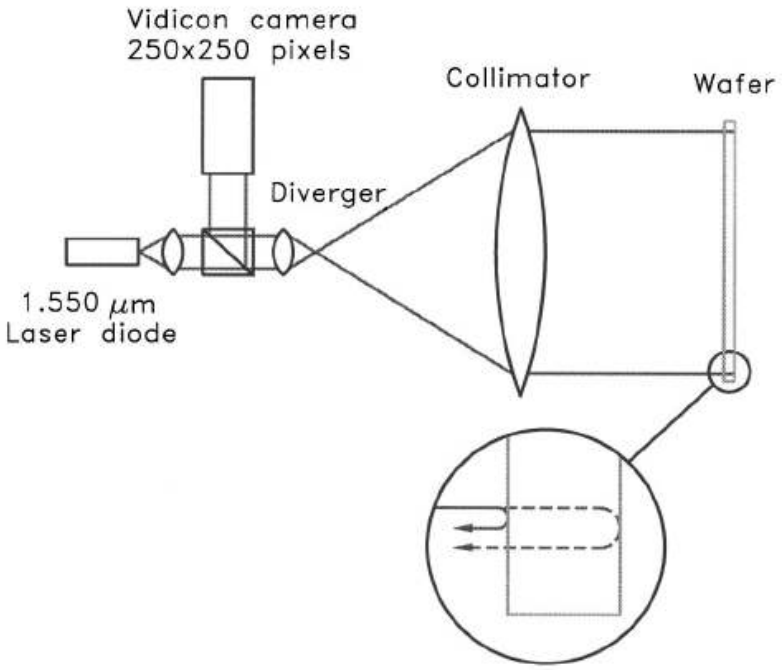

Figure 5: Infrared interferometer in the fizeau configuration [13].

This interferometer is used to measure semiconductor wafers. The light from the tunable IR source is collimated and expanded to cover the area of a wafer. The thickness variation of the wafer can be measured at different locations of the wafer. A similar

interferometer was implemented at UNC Charlotte. Figure 6 illustrates the interferometer in the Twyman-Green configuration utilizing infrared radiation [14].

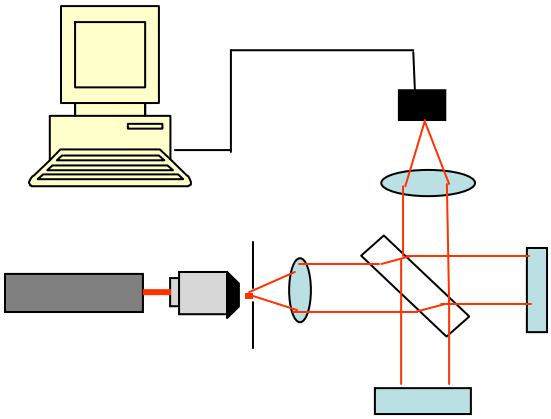

Figure 6: IR Interferometer in the Twyman-Green configuration [14]

A tunable laser is used for this setup. The simplicity of the Twyman Green configuration is the use of a single detector to acquire sample and cavity data resulting in less optics then a Fizeau configuration.

In both of these configurations, the reflection from the back surface needs to be sufficiently specular, as the measurement is based on the spatially coherent interference condition over the area of the wafer. If the surface is rough the interference fringes will not be observed and the measurement is not be possible.

1.5. Non destructive testing using terahertz radiation

Terahertz radiation provides unique advantages over other non destructive techniques. The unique property of terahertz radiation to penetrate insulating material opaque at other wavelengths enables various applications.

The space shuttle tragedy on February 1st 2003 was caused by the detachment of the insulation foam on the shuttle's fuel tank detached and struck off during lift off. Defects on the foam insulation caused the material failure. Of the technologies

investigated for inspection of this defect, terahertz radiation and backscattered X-ray were the most successful. The successful non destructive testing of space shuttle foam material was a very useful application of terahertz quality control [15].

Terahertz metrology has great potential in in-process monitoring of some aspects of the semiconductor manufacturing process. The concept of production line inspection using terahertz radiation has been demonstrated by *Yasui et al* [6]. They successfully designed and implemented a terahertz paintmeter system that was employed to measure the thickness of paint films. They also studied different non destructive testing methods and demonstrated the use of terahertz radiation to measure the thickness of paint films. Voids and other structural ambiguities were identified and the thickness of a paint film deposited on a metal substrate was measured. Figure 7 illustrates the measurement technique they used.

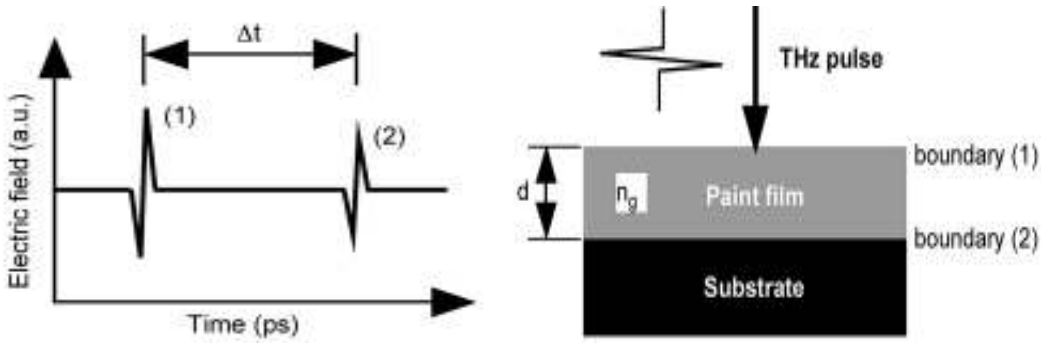

Figure 7: Operating principle of the terahertz paintmeter. The temporal delay between reflected pulses is measured and converted into thickness information [6].

Other technologies such as ultrasonic thickness meters are currently used for this purpose and offer a great degree of portability and reliability. However, such devices perform contact measurements and can be impractical in in-process inspection.

Given these advantages, we decided to design and construct a terahertz time of flight system that could be used for non-destructive measurement applications. In particular, we propose that the method can be used to measure the thickness of single-sided silicon wafers.

CHAPTER 2: TERAHERTZ SOURCES AND DETECTORS

2. 1 Introduction

Terahertz frequencies are too high to be directly approached by microwave technologies and too low for generation by a laser. Until the advent of femtosecond lasers the generation and detection of terahertz radiation was a challenge. Recent advances in terahertz photonics have enabled different types of terahertz sources and detectors. Terahertz sources can be classified based on operational concepts [7].

- Terahertz generation in non linear media.
    - Optical rectification
    - Difference frequency generation
    - Frequency multiplication of microwaves
- Terahertz generation due to accelerating electrons.
    - Transient photoconductive switching
    - Photomixing

Figure 8 Illustrates the different technologies for terahertz generation.

In this chapter we concern ourselves with pulsed terahertz generation methods. A typical pulsed terahertz generation and detection system consists of a pump and probe configuration. The femtosecond laser pulse is divided into two parts using a beam splitter. The pump generates the terahertz radiation while the probe optical pulse goes

through an automated delay line. The terahertz field is obtained by scanning the time delay. In this chapter we will discuss pulsed terahertz technologies.

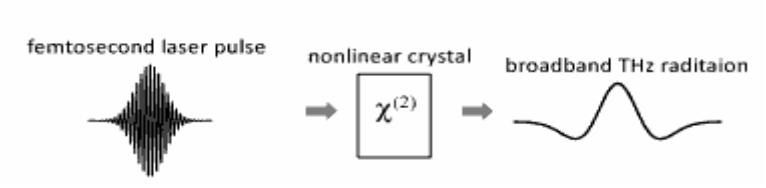

(a) Optical rectification

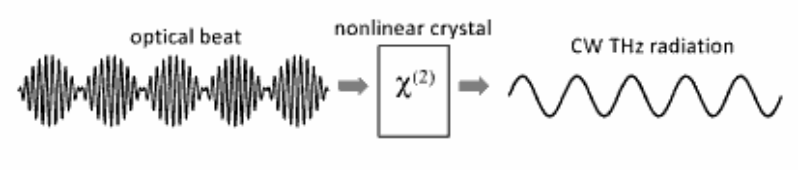

(b) Difference frequency generation

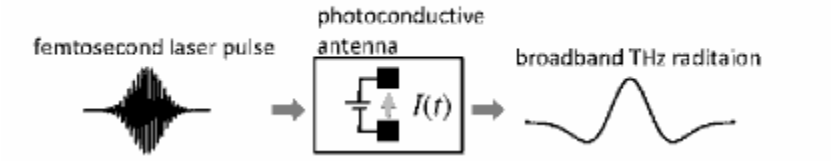

(c) Photoconductive antenna

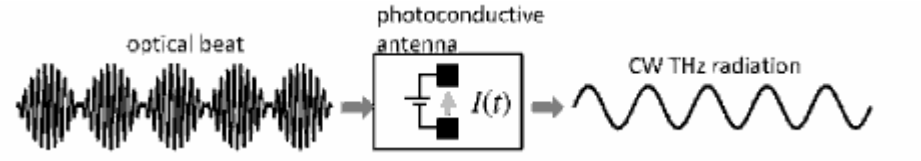

(d) Photomixing

Figure 8: (a), (b) Terahertz generation in non linear media. (c), (d) Terahertz generation from accelerating electrons [7].

2. 2 Terahertz generation by photoconductive antenna

Photoconductive antennas are the most widely used sources for generating terahertz radiation. They are used in most terahertz systems because of the high power

and signal to noise ratio. This section describes the historical development, fundamentals and operating principles of terahertz photoconductive antennas.

2.2.1 Historical development

Experiments by Dr. Heinrich Hertz in 1886 established the Hertzian dipole as a source of electromagnetic radiation [16]. In an attempt to use optical techniques for measuring very fast electronic events, Auston *et al* [17] in 1984 used terahertz pulses to make measurements in the time domain. Their experimental approach was influenced by Hertz's original experiments almost a century ago with dipole radiation, in which he was generating and detecting electromagnetic transients. Two identical photoconductors were fabricated on a single slab of alumina. Both the generator and detector were time varying dipoles. A mode locked ring dye laser was used to illuminate the photoconductors. Figure 9 illustrates the experimental setup for the terahertz generator and detector. The transmitting dipole has a dc bias whereas the receiving dipole receives its bias from the electromagnetic pulse and is connected to a low frequency amplifier. The time response was measured to be 1.6 ps.

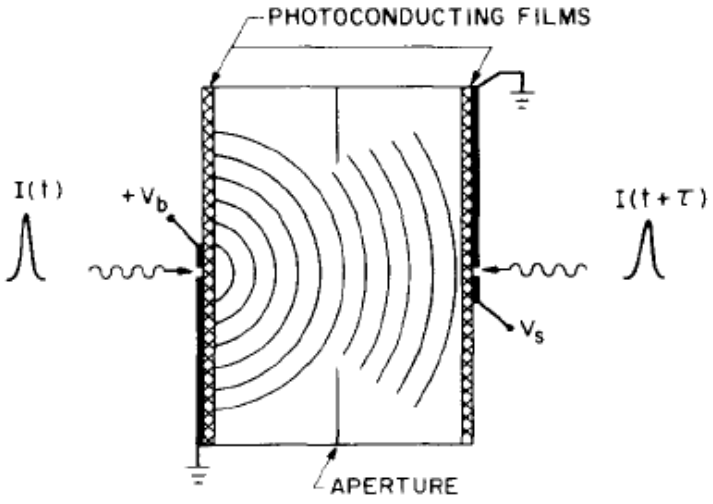

Figure 9: Configuration to generate and detect terahertz pulses [17].

After Auston realized the integrated circuit version of the Hertzian dipole, Grischkowsky and Fattinger [18, 19] demonstrated an optical technique to produce diffraction limited beams of 0.5 terahertz for the first time. Charged coplanar transmission lines were shorted with ultrafast laser pulses and these dipoles were placed at the focus of collimating optics as shown in figure 10. Most of the emitted radiation was captured and focused on detectors. A frequency response exceeding 1 THz was achieved and parabolic mirrors were used for the first time as terahertz imaging optics components.

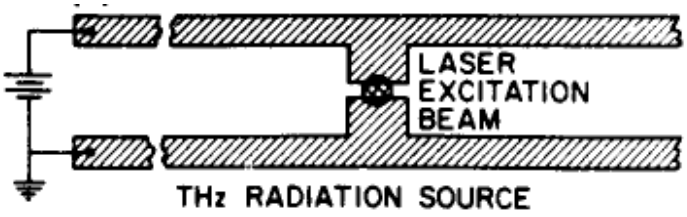

(a) Dipole antenna.

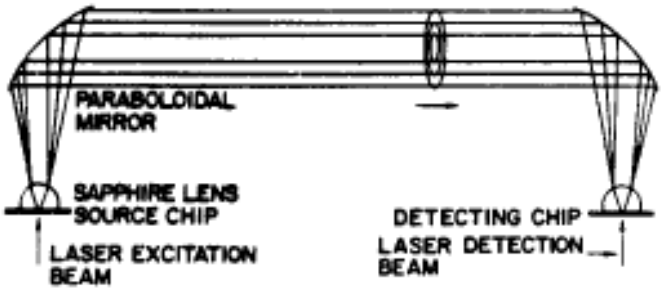

(b) Collimating and focusing optics .

Figure 10: Illustration of terahertz photoconductive antenna used by Grischkowsky [19].

2.2.2 Basic principle

A photoconductive antenna is essentially an electrical switch triggered by increased electrical conductivity of semiconductors when exposed to light. The photon energy of the incident light has to be greater then the band gap of the material. Some important parameters for generation of terahertz radiation from photoconductive antennas are [7]:

- Switching action should occur in the sub picosecond time range.
- Switch on time is a function of the laser pulse; hence short laser pulses are essential for terahertz generation.
- Switch off time is mainly determined by the carrier lifetime in the semiconductor substrate. Short carrier lifetime is a vital property of terahertz generation.
- High carrier mobility is also a desirable feature for photoconductive materials.

Photoconductive antennas are superior to other terahertz generation methods because of their high efficiency and stability. The efficiency of conversion from optical pump power to terahertz emitted power is exemplified by the fact that 10mW optical power from a standard Ti: Sapphire laser oscillator is enough to trigger the photoconductive antenna whereas other sources require orders of magnitude higher pump power [20]. Figure 11 illustrates the basic principle of terahertz generation from a photoconductive antenna.

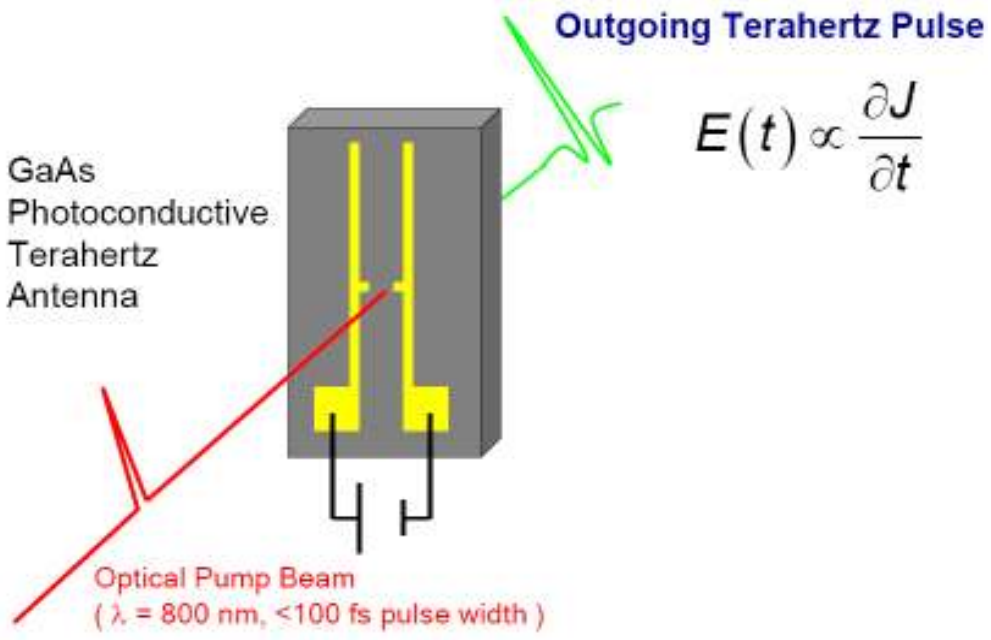

Figure 11: Operating principle of a photoconductive antenna [21].

Table 1 illustrates some advantages and challenges in a photoconductive antenna based terahertz system.

Advantages	Challenges
Near single cycle pulses well delimited in time	Slowly varying amplitude approximations not rigorously applicable
Broad bandwidth pulse allows spectroscopic measurements	Highly absorptive atmospheric water vapor lines limit many field applications
Peak signal-to-noise of detection methods better than 10,000:1 in cases	Low power, on the order of nanowatt average power per pulse
Measurement of electric field phase and amplitude	Requires precise optical beam alignment*
High index-low absorption material (Si) available for optical components	Losses due to reflection at optical interfaces with high index materials
Insensitive to thermal background	
Mesoscopic wavelengths	Scalability of material properties

Table 1: Inherent challenges in photoconductive antenna based terahertz time of flight system [22].

2.2.3. Fundamentals of operation

A Photoconductive (PC) antenna essentially consists of two metal electrodes deposited on a semi insulating semiconductor substrate. A bias voltage is applied across the electrodes which causes electrical energy to be stored in the gap area. Ultrafast laser pulses act like transient switches to create free carriers which are accelerated by the bias field. These accelerating charges produce electromagnetic radiation at terahertz frequency. The current density can be given by the following expression [15]:

$$J(t) = N(t)e\mu E$$

where N(t) is the density of the photocarriers, μ is the mobility of the electrons, and E_b is the bias electric field

The photocarrier density is a function of time and depends on the laser pulse shape and carrier lifetime. Electron mobility is much higher then hole mobility hence contribution of the holes is ignored. Based of Maxwell's equations the emitted terahertz radiation is given by the expressions:

$$E_{THz} = \frac{1}{4\pi\varepsilon_o}\frac{A}{c^2 z}\frac{\partial J(t)}{\partial t}$$

$$E_{THz} = \frac{Ae}{4\pi\varepsilon_o c^2 z}\frac{\partial N(t)}{\partial t}\mu E_b$$

where A is the area of the gap.

The optical excitation triggers the release of the stored energy across the gap. The linear relationships between terahertz emitted radiation and the bias electric field and optical excitation are only true for low excitation and weak bias conditions. Under standard operating conditions the induced terahertz field screens the bias field and the substrate acts as a conductive medium rather then a semi insulating material. The conductivity takes the following form:

$$J(t) = \frac{\sigma(t)E_b}{\frac{\sigma(t)\eta_o}{1+n}+1}$$

where σ is the conductivity and η is the impedance which is 377 Ω for air.

The conductivity is proportional to the laser intensity;

$$\sigma(t) \propto I_o$$

The expression for transmitted terahertz radiation becomes,

$$E_{THz} = \frac{d\sigma(t)}{dt} \frac{1}{\left[1 + \frac{\sigma(t)\eta_o}{1+n}\right]^2}$$

Relating the conductivity to the laser intensity we get the following form

$$E_{THz} \propto \frac{I_o}{(1+kI_o)^2}$$

where $k = \frac{\kappa(t)\eta_o}{(1+n)}$ and κ(t) is the ratio between σ(t) and I_o

Increasing the bias pulse has limitations. Two kinds of dielectric breakdowns can occur in the PC antenna [15]:

1) Field induced breakdown which occurs when the bias field is greater then the breakdown field of the semiconductor (~4 x 10^5 V/cm for GaAs).
2) Thermal breakdown which occurs due to heating of the substrate by photocurrent from the substrate.

The factors effecting PC antenna performance were discussed in detail by Chang *et al* [23]. Following were the main parameters of interest that were explored.

1) Trapping time of charge carriers affects the PC antenna performance. If this time is not short enough terahertz radiation will not be emitted. Terahertz radiation pulses with different trapping times of 0.1,0.2,0.5,1.0 and 2.0 ps were recorded and it was observed that LT-GaAs antennas with longer trapping times can generate higher power terahertz radiation. Figure 12 shows the simulated terahertz response with different trapping times.

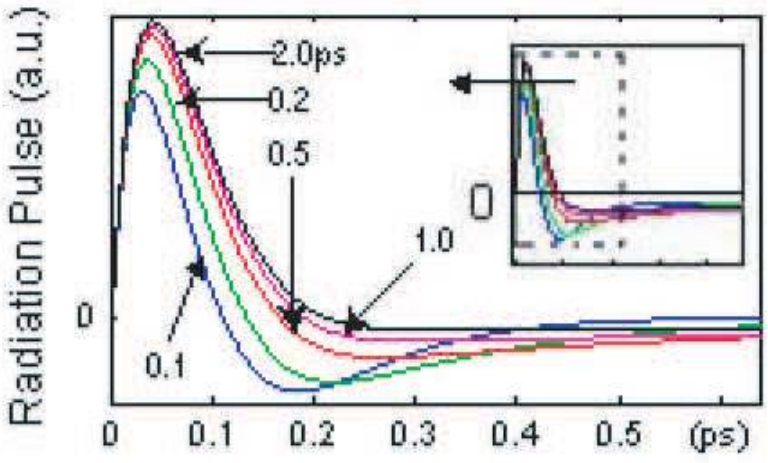

Figure 12: Terahertz radiation pulses with different trapping times [23].

2) Laser pulse duration is another important factor in determining the generation of terahertz pulses. Keeping the trapping time constant at 0.5 ps, and exciting the gap with pulses of wavelengths 620nm and 1550 nm, the terahertz waveform is observed. A frequency domain analysis of the terahertz signal is performed using pulse widths of 50, 100 and 150 ps. Figure 13 illustrates the effect of pulse with and wavelength on the terahertz signal.

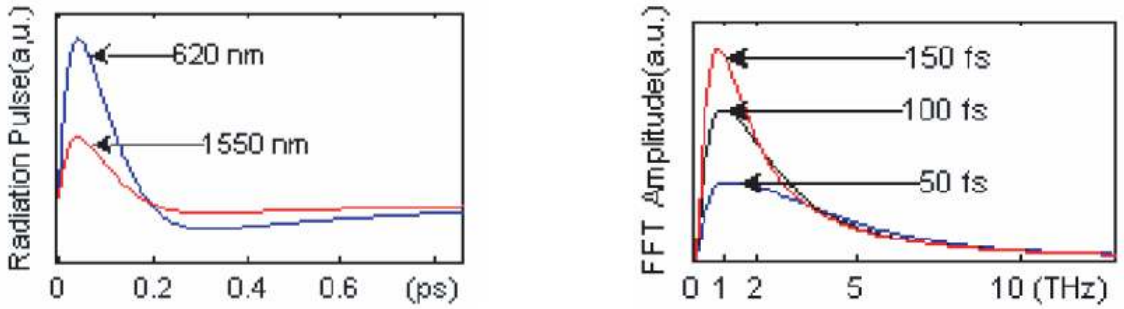

(a) (b)

Figure 13: a) Terahertz radiation pulses with wavelengths of 620 nm and 1550 nm. (b) Frequency domain spectrum of terahertz radiation with different pulse widths [23].

The longer pulse duration and smaller wavelength of the laser generate more powerful THz waves.

3) The effect of the bias field and dipole aperture size is explored. The bias voltage is varied from 200, 300 and 400 V while the gap sizes are varied from 4um, 5um and 7 um. It is observed that greater the bias voltage and smaller the gap, greater is the terahertz emitted radiation. Figure 14 illustrates the effect of bas field and aperture size.

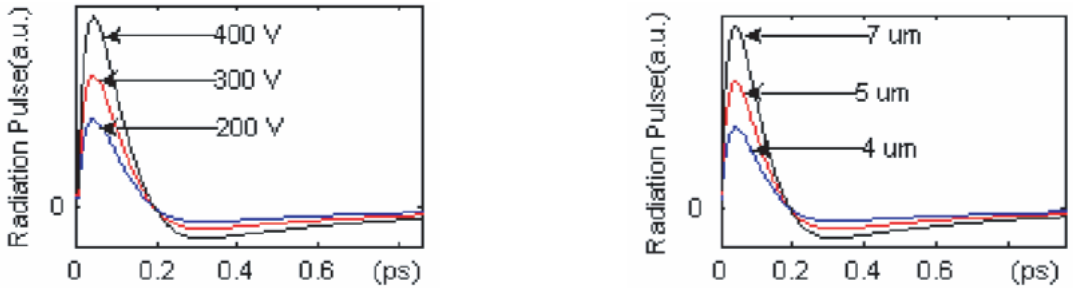

(a) (b)

Figure 14: Terahertz time domain field with (a) different bias voltages, (b) Different gap sizes [23].

2.3 Terahertz generation by optical rectification

The optical rectification technique for generation of terahertz pulses is based on the frequency mixing in an electro-optic crystal. A material with strong non linear coefficient interacts with femtosecond laser pulses and causes difference frequency mixing between various frequencies contained in the bandwidth of the laser pulse. The terahertz fields are low energy single cycle pulses and phase matching requirements between the laser pulse and the generated terahertz radiation make generation of high power pulses difficult.

2.3.1 Historical development

A detailed mathematical expression for the electro optic coefficient of Zinc blende non linear crystals was derived by Namba [24] in 1960. The development of ultrafast lasers made the generation of terahertz radiation from non linear crystals possible. In 1976, Shen and coworkers [25] successfully generated far infra red radiation by illuminating $LiNbO_3$ with a femtosecond laser. Auston and Cheung [26] demonstrated optical rectification of femtosecond optical pulses to produce terahertz radiation using a lithium tantalate non linear crystal. Zhang and coworkers [27-29] reported the generation of terahertz radiation from various non linear crystals using optical rectification and demonstrated their applications using different configurations of terahertz time domain spectrometers.

2.3.2 Operating principle

Terahertz radiation is generated as a result of a second order non linear process. The polarization, represented by P(t), is the dipole moment per unit volume. Polarization is the function of the electric field and represented by the following equation,

$$P(t) = \varepsilon_o \chi^{(1)} E(t)$$

where ε_o is the permittivity of free space and $\chi^{(1)}$ is the linear susceptibility of the material. If the response of a material is non linear, the polarization equation takes the form,

$$P(t) = \varepsilon_o [\chi^{(1)} E(t) + \chi^{(2)} E^2(t) + \chi^{(3)} E(t) + ...]$$

where $\chi^{(2)}$ and $\chi^{(3)}$ are the second and third order non linear susceptibilities respectively. Polarization can also be represented as,

$$P(t) = P^{(1)}(t) + P^{(2)}(t) + P^{(3)}(t) + \ldots$$

where $P^{(2)}(t)$ is the second order non linear polarization represented by,

$$P^{(2)}(t) = \varepsilon_o \chi^{(2)} E^2(t)$$

The second order non linear response occurs only in non-Centro symmetric crystals. Such crystals do not display inversion symmetry. The wave equation in a non linear medium is,

$$\nabla^2 E - \frac{n^2}{c^2}\frac{\partial^2}{\partial t^2}E = \frac{1}{\varepsilon_o c^2}\frac{\partial^2}{\partial t^2}P^{NL}$$

The term $\frac{\partial^2}{\partial t^2}P^{NL}$ represents the acceleration of the constituent charges of a medium. Hence in the above inhomogeneous wave equation, the electric field is driven by the polarization associated with the non linear response of the medium, which is the physical basis for terahertz generation [30].

2.4 Terahertz detection using electro-optic sampling

Electro-optic sampling was first applied for the measurements of ultrafast electrical transients in 1983 by Valdmanis and Marou [31]. They reviewed the theory and applications of the technique. Free space electro-optic sampling measures the amplitude and phase of the terahertz electric field in the time domain. In this method, the change in polarization of an ultrafast probe beam is measured. The measured polarization change can draw an exact picture of the terahertz field. The propagation of optical radiation in a crystal is governed by the impermeability tensor $\eta = \varepsilon_o/\varepsilon$. The ion lattice of a crystal gets

altered when an electric field is applied. The resulting change to the impermeability tensor is called the electro optic effect.

The ellipsoid of the refractive index of Zincblende crystals such as ZnTe when the electric field is applied can be given by the following expression:

$$\frac{x^2 + y^2 + z^2}{n_o^2} + 2\gamma_{41}E_x yz + 2\gamma_{41}E_y zx + 2\gamma_{41}E_z xy = 1$$

where no is the refractive index of the crystal without the electric field and E_x, E_y and E_z are the electric field components along corresponding axes, and γ_{41} is the EO coefficient of the crystal. The phase delay is a function of the refractive index change and is given by the following equation:

$$\Gamma = \frac{2\pi d}{\lambda}\Delta n$$

where d is the thickness of the EO crystal and Δn is the difference in the refractive index. The phase delay for a <110> oriented ZnTe crystal is given by the equation [15]:

$$\Gamma = \frac{\pi d n_o^3 \gamma_{41} E}{\lambda}\sqrt{1 + 3\sin^2\phi}$$

Zinc blende crystals are better suited for terahertz generation and detection because of improved phase matching compared to other crystals. Some important parameters of Zinc blende crystals were studied by Zhang et al [15] and are tabulated in table 2. In the absence of the terahertz field the phase delay is zero keeping the polarization of the probe beam linear. When the terahertz field is present, the phase delay is induced causing the polarization to be slightly elliptical. The polarization analysis of the terahertz electric

field and optical pulse in the sensor crystal provides information on the amplitude and phase of the terahertz pulse.

	ZnTe	GaAs	InP	GaP	ZnS
E_π ($l = 1$ mm) (kV/cm)	89.0	161	153	252	388
Field sensitivity (mV/cm$\sqrt{\text{Hz}}$)	3.20	5.80	5.51	9.07	12.2
NEP (10^{-16}W/Hz)	0.27	0.89	0.80	2.2	5.2
V_{TO} (THz)	5.3	8.0	10.4	11	10.8
$\sqrt{\varepsilon}$	3.18	3.63	3.54	3.34	2.88
N	2.85	3.63	3.54	3.18	2.32
Phase-matching wavelength (nm)	822	1,405	1,230	1,030	470
Frequency of TO photon (THz)	5.3	7.6	10.0	10.8	9.8

Table 2: Electro optic properties of Zincblende structures [15].

Electro-optic sampling is used for terahertz detection. The technique is shown in figure 15. The terahertz electric field and the optical probe beam propagate collinearly in the non linear crystal. The femtosecond optical probe beam is linearly polarized. In the absence of the terahertz field there is no phase retardation in the ZnTe crystal. The quarter wave plate converts the linear polarization to circular. The Wollaston prism (WP) splits the beam into its orthogonal components and sends them to balanced detection electronics.

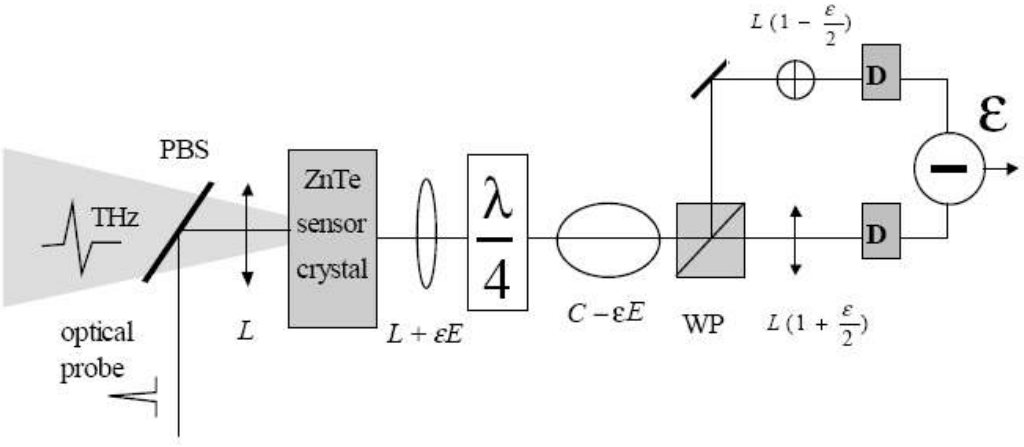

Figure 15: Typical setup for terahertz electro optic sampling [32].

Since the orthogonal components have the same magnitude for a circular polarized beam, the difference should be close to zero. When the terahertz field propagates in the crystal with the femtosecond beam, it induces birefringence causing the polarization to be elliptical. The variable ε, is the fraction of elliptical polarization induced. The linearly polarized optical beam is converted to an elliptically polarized beam. This fractional change in ellipticity manifests itself as a change in the difference voltage. The terahertz field is extracted using a lock in amplifier.

The detection scheme depends on the angle of the electro optic crystal relative to the terahertz electric field. The angle between the space coordinates and crystallographic axis of the crystal in space is known as the azimuthal angle. For the maximum terahertz signal, the polarization of the probe beam and terahertz electric field are parallel to the <110> direction of the ZnTe crystal in the electro optic sampling method [7]. Figure 16 illustrates this behavior.

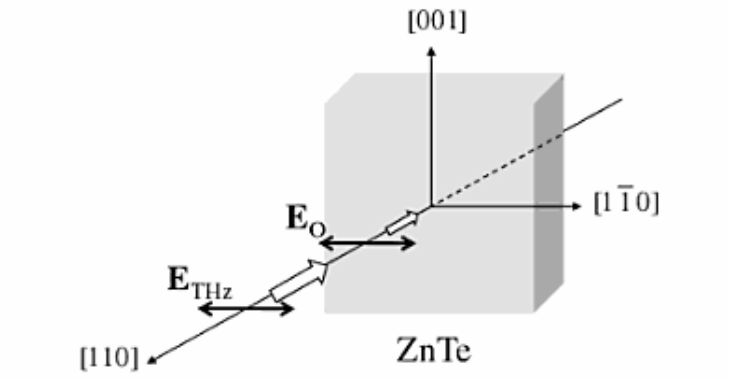

Figure 16: Relative positions of the probe and pump beams for maximum terahertz signal [7].

For birefringent crystals there are two polarization directions which are solutions to Maxwell's equation. These are called the propagation modes of the crystal [33]. This description is true for electro-optic detection where birefringence is caused by the

terahertz electric field. Zhang *et al* [15] formulate an expression for the s and p polarization states in terms of the optical coefficients of the crystal and orientation of the excitation pulse

$$P_{\parallel} = \frac{3}{4}\varepsilon_o d_{14} E^2 \left(\cos 3\theta - \cos\theta\right) \text{ and}$$

$$P_{\perp} = \frac{1}{4}\varepsilon_o d_{14} E^2 \left(3\cos 3\theta + \cos\theta\right)$$

The azimuthal angle dependence is show in figure 17

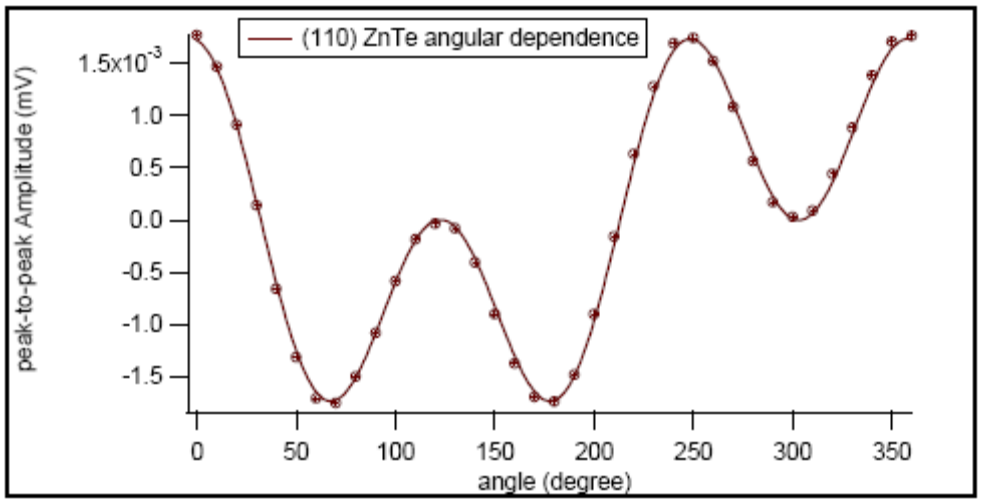

Figure 17: Angular dependence of <110> ZnTe crystal [34]

2.5 Terahertz detection from photoconductive sampling

The use of photoconductive antenna as the terahertz detector is similar to the use of the PC antenna as an emitter. The electrodes are connected to a current sensor and the optical probe beam creates photocarriers. Figure 18 shows the PC sampling setup. The photocarriers are generated in the substrate material. If at the same time the terahertz field reaches the detector, the photocarriers are driven by the electric field.

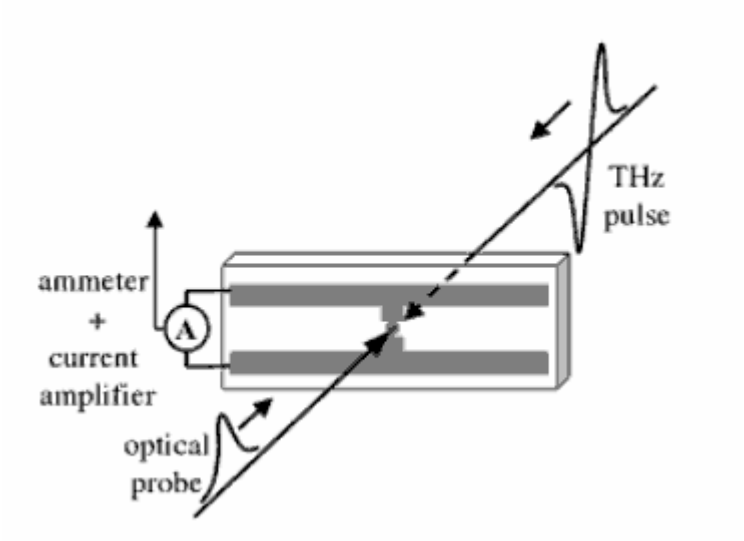

Figure 18: Terahertz pulse detection from PC antenna [7].

For a time delay τ, the induced photocurrent is given by the following expression [20]

$$i_{THz}(\tau) \propto \int G(t-\tau) E_{THz}(t) dt$$

where G(t) is the transient photoconductance of the antenna. The equation illustrates that the detection bandwidth is limited by the carrier dynamics of the material. The lifetime of the carriers should be much shorter then the terahertz pulse. This enables the photoconductive switch to sample the terahertz field at a shorter duration of time [35].

2.6 Comparison of EO sampling and PC Sampling

Terahertz waveforms obtained from electro optic sampling and photoconductive sampling were compared by Park *et al* [36]. Three different kinds of emitters were used to generate terahertz radiation. The resultant waveforms were measured and compared using the free space EO sampling and PC antenna sampling. Figure 19 illustrates the resultant signal. It is clear that different emitters produce different terahertz waveforms. The dotted line in the PC sampling waveforms is the calculated signal whereas the sold line is the measured signal.

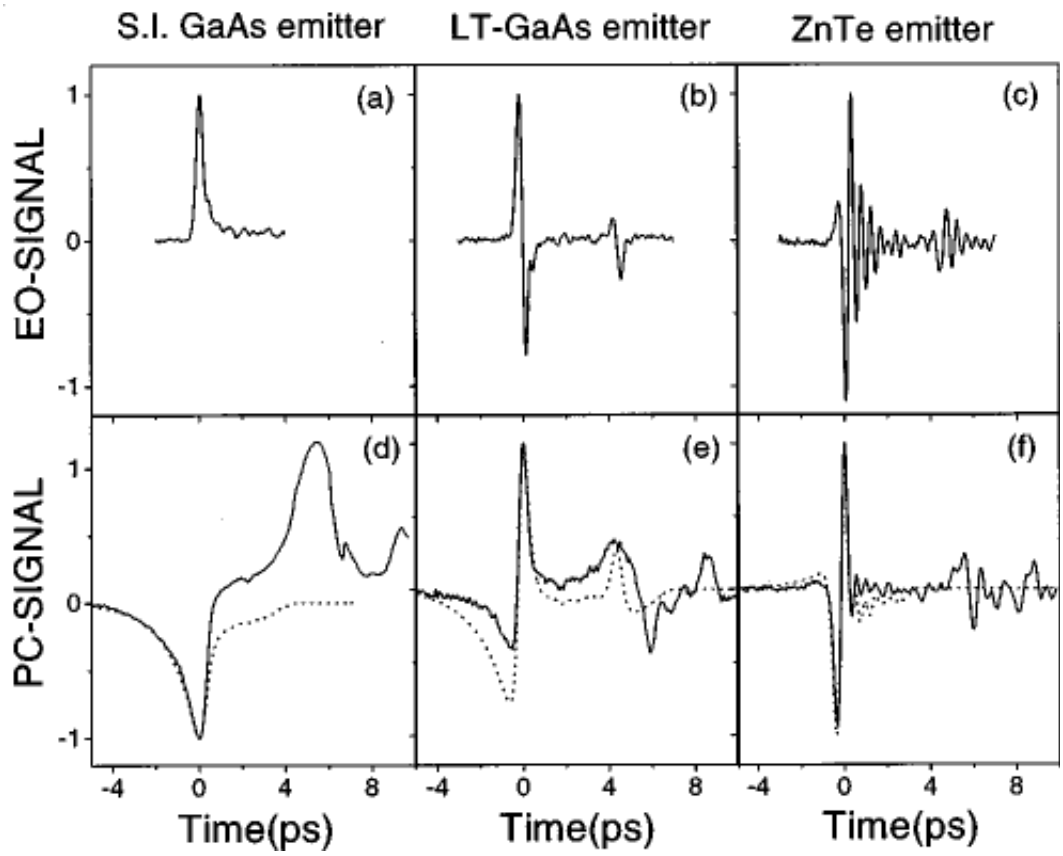

Figure 19: Terahertz signal from PC sampling and EO sampling [36].

The carrier lifetime and frequency dependant response of the PC antenna explains the difference in the measured waveforms using the two techniques [36]. Sine free space EO sampling is independent of these effects, it gives a more true picture of the terahertz waveform.

CHAPTER 3: TERAHERTZ SYSTEM DESIGN AND IMPLEMENTATION

3. 1 Terahertz systems

As a result of the growing interest in terahertz radiation, a multitude of system configurations have emerged for various applications in terahertz research and development. A lot of interest lies in security applications. Terahertz systems optimized for use in security are calibrated for greater standoff distances. Such system designs have been realized and cited in the literature [37-39]. Terahertz systems are sometimes characterized by the source and detector technology used. Continuous wave terahertz systems make use of photomixers for terahertz generation and bolometers for detection [40]. Terahertz detection has also been successfully realized using CCD cameras. In such detection schemes, a pair of crossed polarizers is used. The output probe beam is divided into two parts, the terahertz beam and a coherent background and it is possible to measure the terahertz beam as long as the terahertz signal beam is weaker then the background [41-42].

The first demonstration of a terahertz imaging system for non destructive testing was done by Hu and Nuss [43] at AT&T and Bell labs. They used photoconductive antennas as a source and detector of terahertz radiation. A mode locked Ti: Sapphire laser at a wavelength of 800 nm was used to excite the photoconductive antenna. Other research groups independently demonstrated the applications of terahertz radiation using different

configurations. A commonly used design was the use a photoconductive antenna to generate terahertz radiation and a non linear electro-optic crystal for terahertz detection [44]. Such a measurement technique enabled the true terahertz waveform to be extracted from the signal eliminating the need for electrical contact with the sensor crystal [29]. The terahertz photonics lab at the University of Osaka has successfully employed similar configurations for applications in non destructive testing applications [6, 45-46].

3. 2 Design considerations

Our research focus is on applications of terahertz radiation in metrology. Our goal is to develop a terahertz metrology system using a pulsed laser. Our primary objective is to measure a metal object embedded in an insulating material and demonstrate our ability to measure the thickness of a subsurface structure or the thickness of a sample using a time of flight configuration. We leveraged our expertise in interferometery and optical test methods to develop measurement configurations and methods.

3. 3 Terahertz metrology system

3.3. 1 Overview

Our terahertz metrology system would is able to map the dimensions of a subsurface structure and perform a detailed uncertainty analysis by analyzing the data.

The penetration of AC electric fields inside conductors is called skin depth. The following equation is an expression for skin depth [47].

$$\delta = \sqrt{\frac{2\rho}{2\pi f \mu_r \mu_o}}$$

Where, ρ = resistivity,f = frequency, $\mu_o = 4\pi \times 10^{-7}$ Table 3 shows the skin depths of different materials at a frequency of 1 terahertz. Since terahertz radiation does not

penetrate appreciable lengths inside metals, we would not be able to use our terahertz metrology system to measure metallic substances. The skin depth of terahertz radiation for undoped silicon wafers is over 12 mm. Since the typical thickness of silicon wafers ranges from 300 to 400 microns, terahertz time domain imaging systems can easily probe silicon wafers and measure absolute.

Material	**Skin depth (μm)**
Aluminum	0.08
Copper	0.07
Gold	0.08
Nickel	0.15
Titanium	0.37
Silicon (un-doped)	12,732
Germanium (un-doped)	341

Table 3: Skin depth of materials at 1 THz.

The terahertz metrology system is designed to be capable of measuring the following,

- Thickness of silicon wafers.
- Thickness of paint films.
- Substrate material in semiconductor manufacturing technology.
- Thickness of optically opaque dielectric material (cardboard, packing material etc.).

3.3. 2 System components

The terahertz metrology system is designed as a typical terahertz time of flight spectrometer. Measurements can be made in either transmission or reflection geometry

depending on the type of sample being measured. Figure 20 illustrates the essential components of the terahertz metrology system.

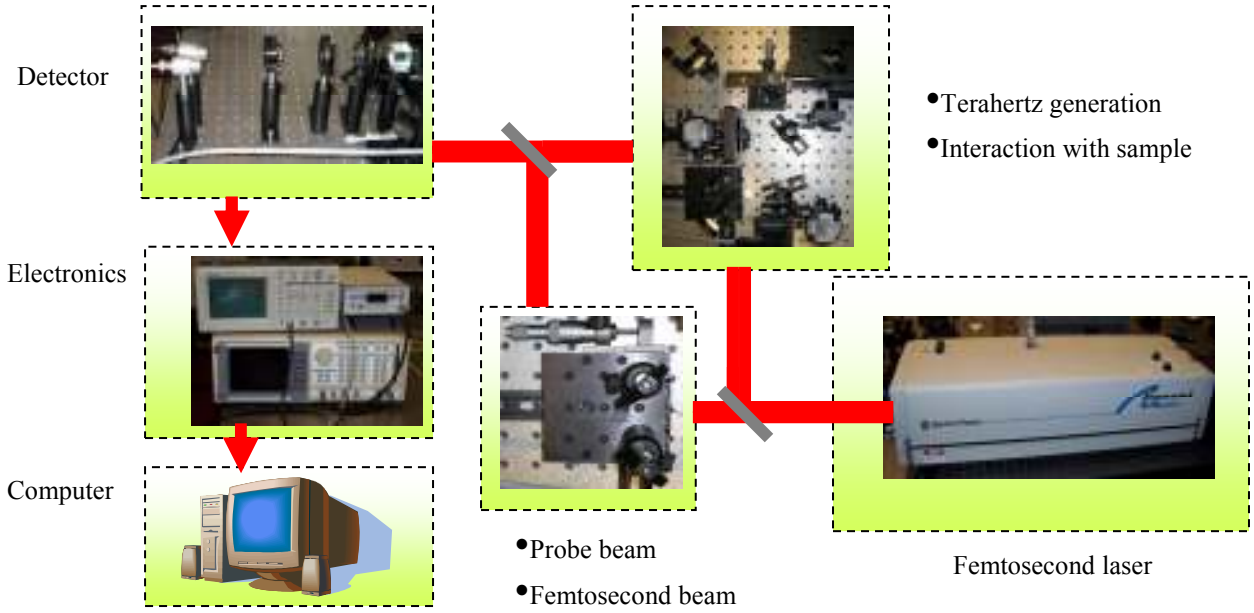

Figure 20: Terahertz metrology system.

The fundamental components of the terahertz system are, femtosecond laser, terahertz source, terahertz beam optics, terahertz detector.

The femtosecond laser pulses are split by the beam splitter. The stronger portion of the beam called the pump beam is focused on the terahertz source antenna by an achromatic lens. The terahertz radiation generated is used to probe the sample in the desired configuration (e.g transmission), then the terahertz is collimated and focused using off axis parabolic mirrors on the terahertz detector crystal. The weaker femtosecond laser pulse is incident at the terahertz detector crystal after passing through a computer controlled mechanical optical delay line. The terahertz pulse is sampled using the weaker femtosecond pulses through a balanced detection setup. The data is recorded

and analyzed using Labview software. Each component is described in more detail below.

3.3.2. 1 Femtosecond laser

The femtosecond laser is an integral component of the terahertz system. It is used to generate the terahertz radiation by focusing it on the terahertz photoconductive antenna. We use the Tsunami mode lock Ti: Sapphire laser by "Spectra-Physics". It is a solid state laser and can be tuned over a broad range in the near infra red spectrum. The major components of the laser are Ti: Sapphire laser head, electronics module, regulator unit, chiller and the beam routing optics [48].

The pump for the femtosecond laser is the "Millennia V" Nd: YAG laser also from spectra-physics. The pump laser operates at a wavelength of 532 nm and 5W power. The femtosecond laser is set to a wavelength of 800 nm and a repetition rate of 80 MHz. Figure 21 illustrates the system interconnect block diagram for the femtosecond laser.

All safety precautions must be undertaken when operating both the Millennia and the Tsunami laser. Both the lasers are classified as class IV and are capable of causing permanent damage to the human eye by exposure of either direct or scattered beams. The beam should be attenuated during alignment and everyone in the vicinity at risk of exposure should wear laser goggles with OD>7 at 800nm. It should always be known where the beam is going before letting it go there. The beam should be maintained at the table height and the operator should not reach down if an object is dropped. The chiller unit is turned on before activating the pump laser. We make sure the laser is at a suitable temperature and and turn on the pump laser after a around ten minutes. The laser warms up and stabilizes the diode temperature. The laser needs a warm up period of around half

an hour [49]. Mode locking should be ensured using an oscilloscope to view the femtosecond pulses. The femtosecond laser is nitrogen purged and the internal optics optimized for maximum efficiency. Once the laser mode locking is ensured, press the mode lock button on the laser control unit to lock the pulse.

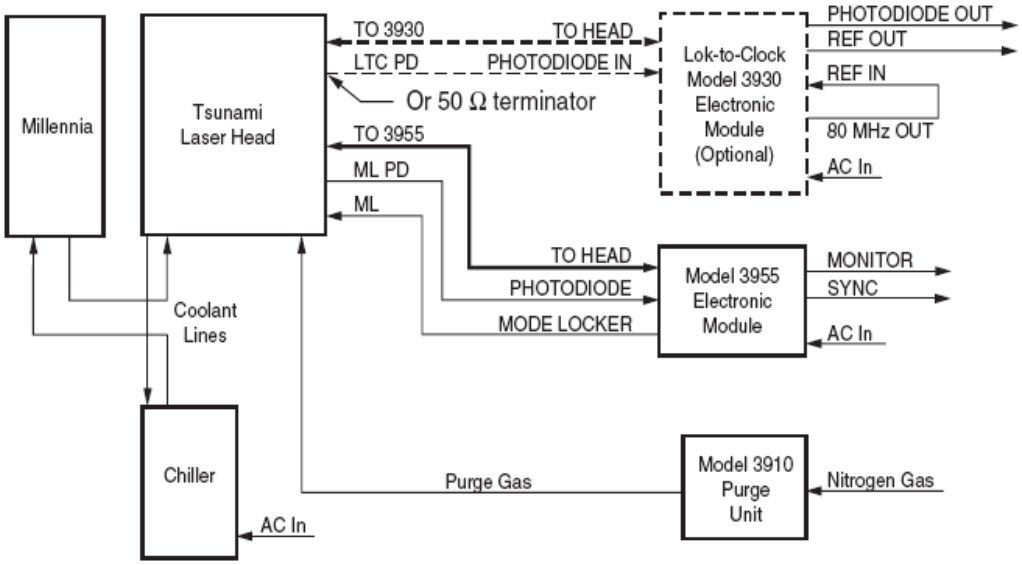

Figure 21: System interconnect diagram [48].

3.3.2. 2 Terahertz source

The terahertz source is one of the most critical components to realize in the terahertz metrology setup. Traditional semiconductor sources cannot operate at these wavelengths due to a variety of reasons. Optical sources operate at low energy levels which makes terahertz generation by these methods impossible without the use of cryogenic cooling. Frequency mixing techniques have successfully been used to generate terahertz radiation using lasers [50]. Terahertz sources are discussed in detail earlier in chapter 2. As discussed earlier, the two main sources for terahertz generation are the photoconductive antenna and the non linear crystal. Our terahertz time of flight system uses a photoconductive antenna as the terahertz source. The photoconductive dipole

antennas use transient photoconductivity for the generation of terahertz radiation. The terahertz source for our system was provided by Zomega Terahertz Corporation. The antenna configuration is shown in figure 21.

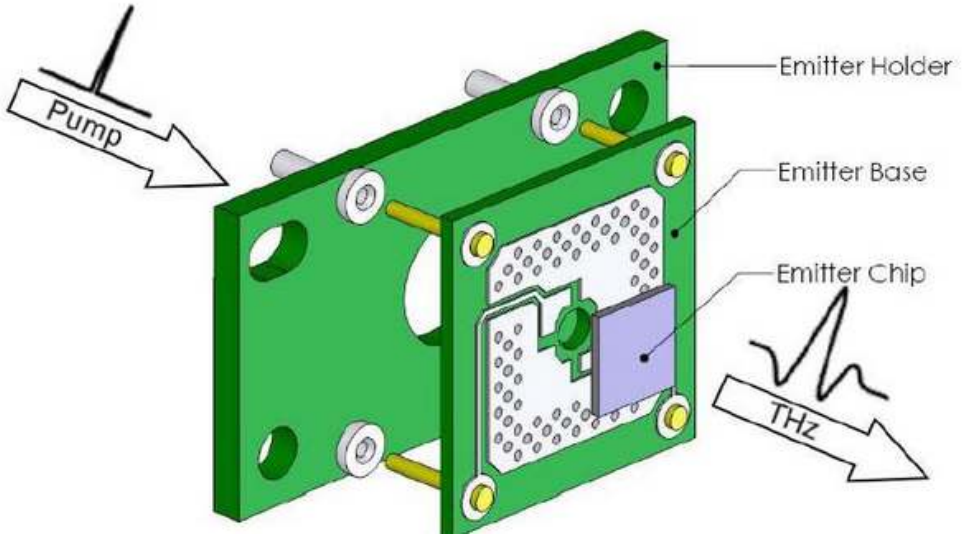

Figure 22: Photoconductive antenna placement.

The antenna was a strip line antenna structure fabricated on a GaAs substrate. The gap width between the two metal leads was 150 μm. The antenna is biased with a high voltage modulator at a frequency of 10 kHz from a function generator. The bias voltage can be set from 70V to 90V. During the alignment process, the antenna is placed at the focal point of the femtosecond source and then translated into focus by a linear translation stage to avoid laser damage. Figure 23 shows the alignment process.

3.3.2. 3 Terahertz beam optics

A high performance terahertz system should possess two fundamental qualities,

- It should permit focusing of the terahertz waves to a diffraction limited spot size.
- It should permit maximum throughput.

The wavelength of terahertz radiation is not negligible as compared to the optical elements used. As a result diffraction effects have a significant contribution in ray

propagation [51]. Reflective components are preferable for beam shaping and propagation.

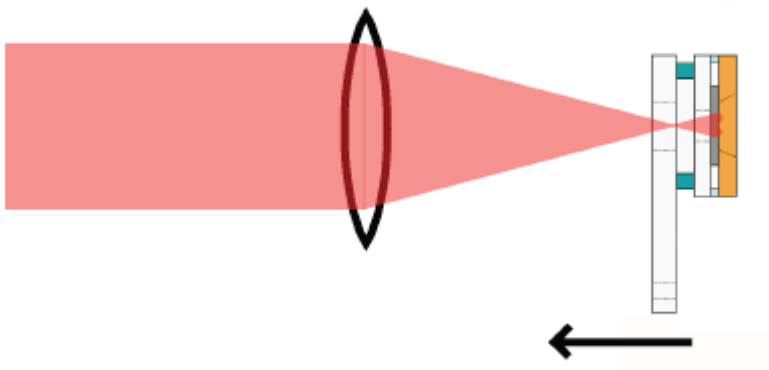

Figure 23: Antenna brought into focus by linear stage to avoid laser damage.

3.3.2.3.1 Parabolic mirrors

Bruckner et al [52] studied the optimal arrangement of parabolic mirrors for terahertz setups. They used ZEMAX optical design software was used to analyze the different configurations. They reported that two off axis parabola mirrors arranged such that the axes of the parent parabolas coincide cancels out astigmatism but introduces distortion. If the arrangement is such that the axes are 180^{o} about their common optical axis, the astigmatism is at the highest but distortion is cancelled out. Hence the ideal arrangement is two off axis parabolas with coincident axes of parent parabolas. Figure 24. Illustrates the optimal arrangement for the off axis parabolas in a typical terahertz setup. Conventional lenses and beam splitters can be used for the femtosecond laser centered at a wavelength of 800nm. However, terahertz radiation is invisible to the human eye and conventional lenses cannot be used for focusing and collimating terahertz beams. In order to focus and collimate terahertz beams we use aspheric mirrors. Off axis parabolic mirrors are used in most terahertz configurations. The femtosecond and the

terahertz beam paths are collinear and the off axis parabolic mirrors are wavelength independent. Hence the optical alignment achieved using the femtosecond laser would apply to the terahertz radiation as well. The generated terahertz radiation from the photoconductive antenna source diverges and is collected by the first off axis parabola mirror.

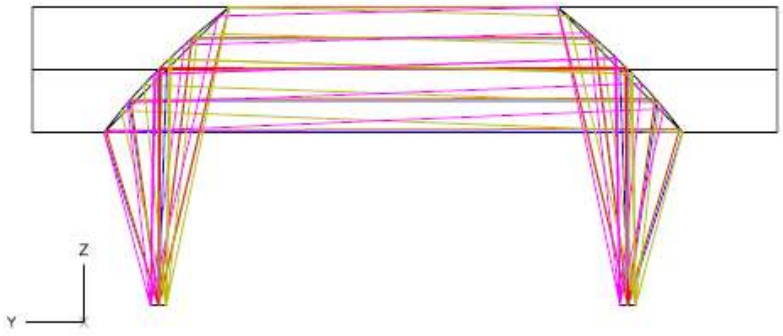

Figure 24: Two off axis parabolas with coinciding axes of parent parabolas modeled using ZEMAX software [51].

The beam splitter used to recombine the beams is the pellicle beam splitter. It transmits the terahertz radiation and reflects the femtosecond optical beam. Figure 25 shows the optical beam setup for the terahertz path.

3.3.2.3.2 Optical delay line

A beam splitter divides the femtosecond laser into a pump beam and a probe beam. The optical probe beam essentially traverses an optical delay line before being reflected to the terahertz detector crystal. The pump beam is used to generate the terahertz radiation through the photoconductive antenna and interacts with the sample to be measured. It is crucial for the two optical paths to be equal for terahertz detection. The detection technique for terahertz detection is free space electro optic sampling and fundamentally depends on the interaction of terahertz pulses and the femtosecond pulses

in a ZnTe crystal. The width of femtosecond laser pulse is set to be 38 femtosecond. From literature, the estimated width of the terahertz pulse is 0.35 picoseconds [29]. Hence the femtosecond laser pulse is much smaller then the terahertz pulse. The femtosecond optical pulses are used to measure the wider terahertz pulse.

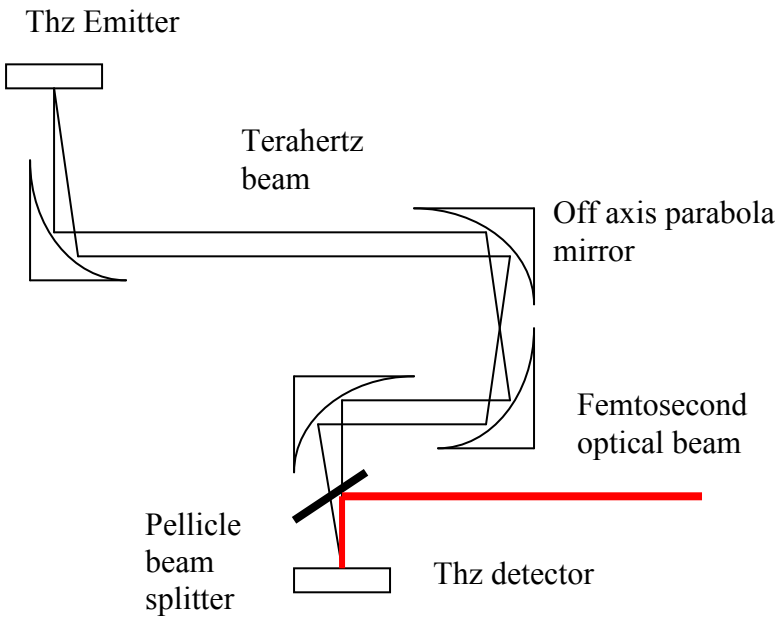

Figure 25: Terahertz beam shaping with off axis parabolic mirrors

The step size of the delay line movement determines the spectral resolution of the terahertz system. The following equation quantifies the spectral resolution:

$$\Delta v = \frac{1}{N\Delta t}$$

Where N is the number of data points and Δt is the time delay.

In order to get a better perspective of the relative dimensions in terms of time and displacement, we use the following equation to relate the time step to the spatial movement of the motorized stage:

$$\Delta t = \frac{2\Delta x}{c}$$

where Δx is the physical displacement, Δt is the temporal width and c is the speed of light. Figure 26 is an illustration of the femtosecond and terahertz optical pulses. We also consider all units in picoseconds for the sake of uniformity. As an example, a 100fs optical pulse corresponds to 0.1 picoseconds and an equivalent width of 15 microns. Hence we infer that a 15 micron translation equates to the movement of the femtosecond pulse by 0.1 picoseconds. Since the equivalent width of the terahertz pulse is 1.5 mm, the femtosecond pulse can be translated to obtain 100 samples which would scan the entire terahertz pulse. The repetition rate of the femtosecond laser is 80 MHz, which means that the next femtosecond pulse would occur after 10,000 picoseconds, or equivalently 3 meters. One femtosecond pulse generates one terahertz pulse from the photoconductive antenna. Hence it is critical for the femtosecond pulses to co-propagate in the ZnTe detector crystal in the presence of the terahertz field. This proves that the pump and probe paths need to be equal to within the pulse width of the terahertz electric field. This can be achieved by measuring the two propagation paths and making them as equal as possible and adding an automated optical delay line which is capable of scanning in steps no larger then 3 microns. Figure 27 illustrates the sampling of the terahertz signal by a femtosecond optical pulse. A single femtosecond pulse generates one terahertz pulse. Identical copies of the femtosecond pulse, and hence the terahertz pulse, are produced at the repetition rate of the laser. Making the two optical path lengths equal ensures that each terahertz pulse interacts with the corresponding femtosecond pulse. By translating

the delay line we look at a different set of identical pulses. Hence we are not looking at a single pulse but the average shape of many terahertz pulses [53].

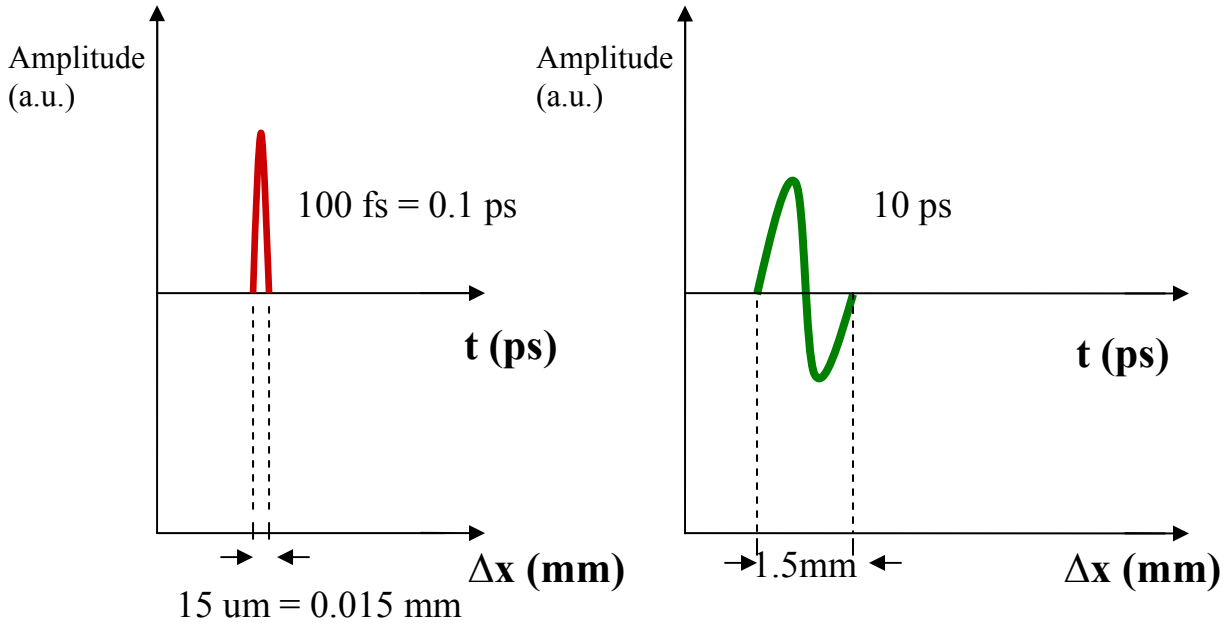

Figure 26: Comparison of terahertz and femtosecond pulses.

In Figure 27, waveform (a) is the terahertz wave that we wish to measure. Waveform (b) is the corresponding femtosecond optical pulse. The femtosecond pulse can be scanned or delayed in time using the optical delay line. Waveform (c) is the measured waveform obtained by sampling the terahertz pulse with the femtosecond pulse. The measured waveform is a function of the generated terahertz pulse. Two mirrors in the retro reflector configuration were mounted on a linear translation stage. A motorized actuator was connected to the translation stage and controlled through the computer.

The actuator used was the “Newport 850G single axis actuator”. The maximum travel on the actuator is 50 mm with a step size of 2.5 μm [54]. The motor is controlled

through the “SMC 100CC” controller also by Newport corporation. The controller requires an encoder adapter to interface with the motor. Communication with the controller is through RS232 . Labview software is used to program the motor to move the stage to the desired displacement.

3.3. 3 Terahertz detector configuration

The lack of detectors in the terahertz frequency is a major limitation in terahertz systems. One of the fundamental reasons for this the low photon energies at these frequencies which allow ambient noise to dominate. Longer wavelength detection techniques cannot be used because of the lack of available components [50]. The physics of terahertz detection by electro optic sampling has been discussed in detail in chapter 2. Free space electro optic sampling is used to detect terahertz radiation in our system. The process is very sensitive and can extract the true waveform of the terahertz electric field. A critical requirement for successful detection of a terahertz pulse in a non linear crystal is the phase matching between the generating and detecting crystals. Thin non linear crystals provide good phase matching at terahertz frequencies. The generation and detection crystals may exhibit etalon effects. Terahertz back reflections inside the crystal appear in the time domain scans at intervals equal to,

$$\Delta T_{etalon} = \frac{2 n_g d}{c}$$

where n_g is the group refractive index and d is is the crystal thickness. The fringes produced as a result will be of the frequency,

$$\Delta f_{fringe} = \frac{1}{\Delta T_{etalon}}$$

A crystal with thickness of 1 mm, laser wavelength of 800 nm and terahertz refractive index n_g of 3.1 will have fringes at 20.6 ps intervals. To counter this phenomenon the measurement time has to be less than ΔT_{etalon}. Strong oscillations caused by etalon reflections cause oscillations in the dynamic range of the system [55].

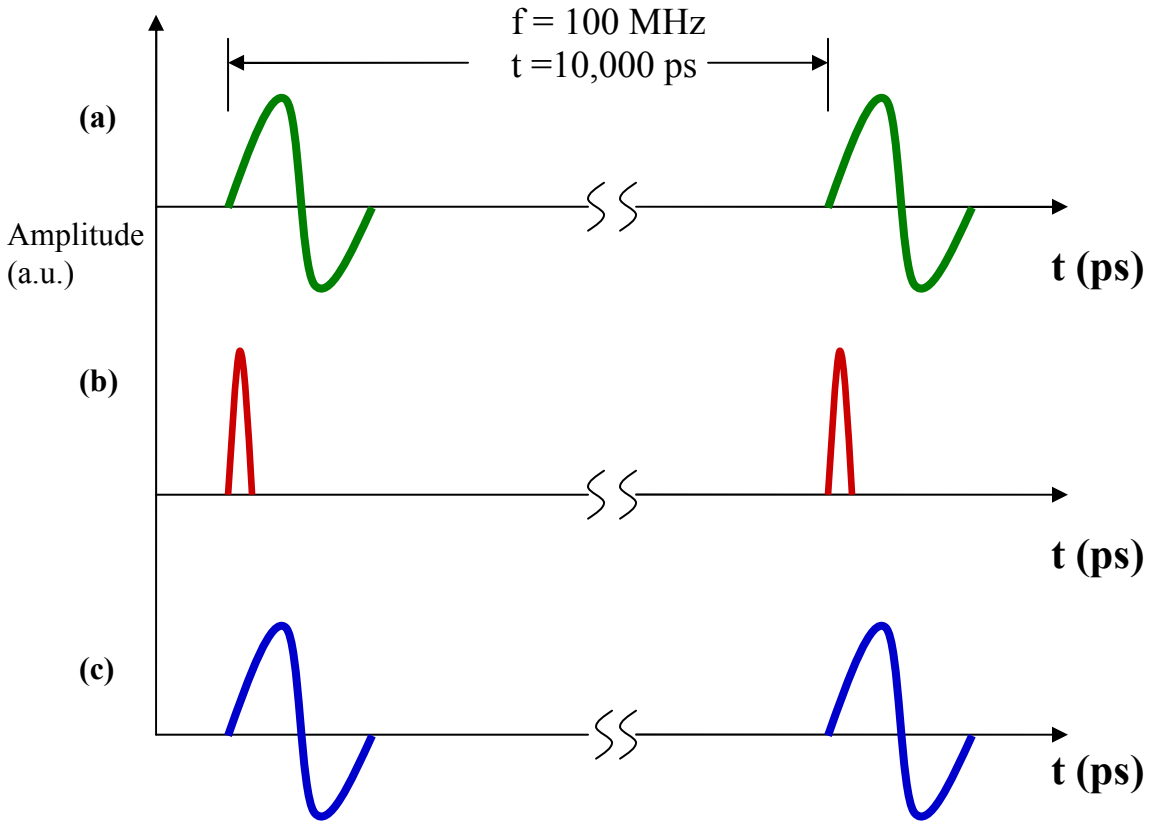

Figure 27: Sampling of terahertz waveform by femtosecond laser pulse. (a) Terahertz waveform. (b) corresponding femtosecond optical pulse. (c) measured terahertz waveform obtained by sampling (a) and (b).

The detection method employs the Pockels effect in an electro optic crystal which is a ZnTe crystal in our case. A quarter wave plate equalizes the amplitudes of the orthogonal components of the femtosecond beam and sets the polarization as circular.

The femtosecond and terahertz pulse are coincident inside the crystal. The presence of the terahertz field changes the birefringence of the crystal causing a change in polarization of the femtosecond beam to elliptical. The orthogonal polarization components are split using a Wollaston prism and sent to photodiodes. The difference signal is sent to the lock in amplifier which measures the change in polarization caused by the terahertz electric field. The lock in amplifier is synchronized with the computer through GPIB. The results are analyzed by a program written using Labview software. Figure 28 illustrates the terahertz detection setup.

3. 4 System optimization and debugging

It is essential to optimize the design of the terahertz metrology system before experimental implementation. A rigorous study was conducted to examine every element in the system to ensure the best possible performance. The key components of the system that were studied are listed below.

- Orientation of the terahertz detector crystal.
- Interaction of terahertz beam with sample.
- Relative strength of probe and pump optical beams.
- Electronic balanced detection system optimization.

In order to aid the study, a research visit to the terahertz research center at the Rensselaer Polytechnic Institute in Troy, New York was organized. The host center is home to five state of the art terahertz labs [56]. The research being conducted by Dr. Xi-Cheng Zhang and his associates with terahertz radiation systems was observed and discussed. The following conclusions were derived for improving our terahertz metrology system.

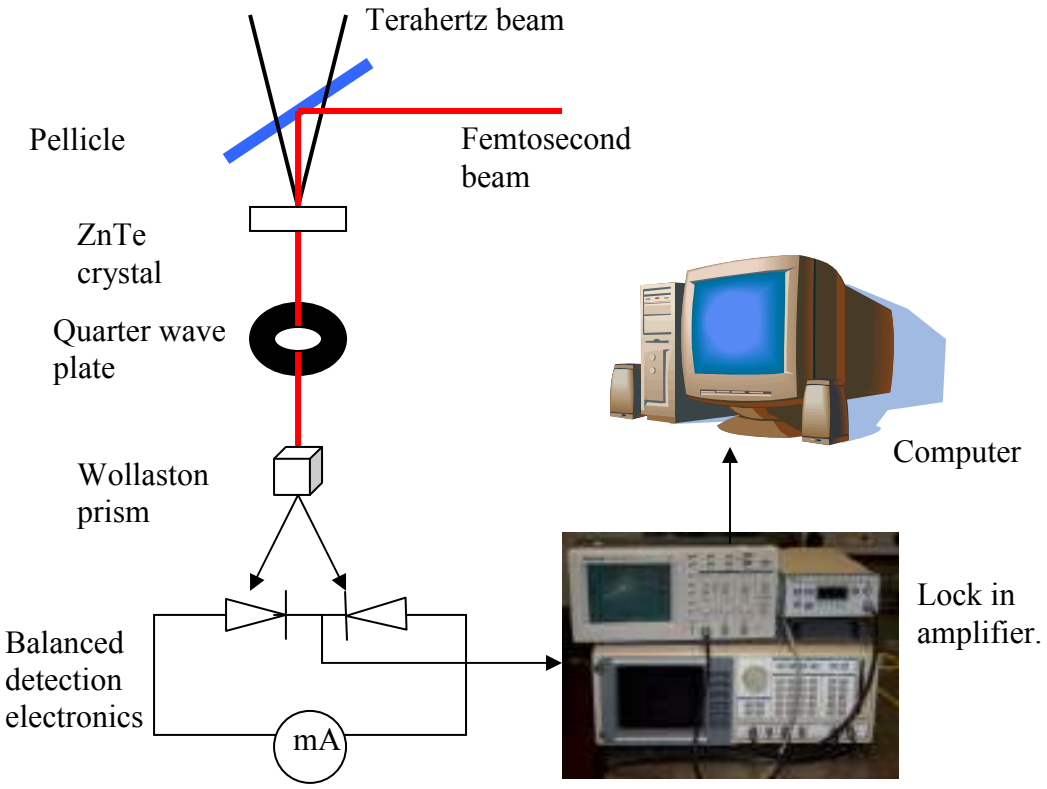

Figure 28: Terahertz detection setup.

3.4. 1 Orientation of the terahertz source and detector crystal.

The orientation of the ZnTe crystal for terahertz generation and detection is critical for optimum performance of the system. The angular dependence of the non linear crystal on the azimuthal angle is described in Chapter 2. Practically, the best method to achieve the correct orientation is to orient one edge of the detector crystal parallel to the optical table while the terahertz generation crystal is rotated in the four possible orientations. When the terahertz signal is detected, finer adjustments can be made by rotation the terahertz generation crystal in smaller steps for an optimal terahertz signal.

3.4. 2 Interaction of terahertz pulses with the measured sample

The measured sample is placed between the two off axis parabola mirrors. The terahertz beam is collimated. Since undoped silicon wafers absorb light in the femtosecond optical regime and transmit the terahertz radiation, we place a silicon wafer in the beam path. This way the femtosecond pulses have no impact on the measured terahertz signal. The terahertz beam and the femtosecond laser are collinear hence, even though we cannot observe terahertz radiation, the terahertz beam and the optical beam are collinear. We use the path of the laser as a guide to the behavior of the terahertz beam.

3.4. 3 Relative strength of the probe and pump beams.

The beam splitter divides the input femtosecond beam into a probe and a pump pulse as previously stated. It is critical for the pump beam to not saturate the photodetector circuit. In order to achieve this, the pump beam should have a greater intensity than the probe beam. More than 90% of the femtosecond pulse intensity should be incident on photoconductive antenna for maximum terahertz signal. The specifications for the photoconductive antenna allow a maximum power of 400 mW to be supplied to the gap between the metallic leads. It is observed that a power of 200mW is sufficient to generate an strong terahertz signal. The current in the photodiodes should optimally be maintained to less then 1mA in order to achieve the best sensitivity. For safety purposes, the femtosecond beam should always be attenuated before any alignment step.

3.4. 4 Electronic balanced detection system optimization.

An important requirement for measuring the terahertz signal is to use balance detection electronics. The difference current should be measured and recorded. One possibility is to use the lockin amplifier in the difference voltage configuration. In this method the photodiode voltages are input to the lock in amplifier. However using this

configuration may add noise to the system. Both the cables need to be of the same length. Figure 29 shows the internal system diagram of the lock in amplifier input in difference voltage configuration.

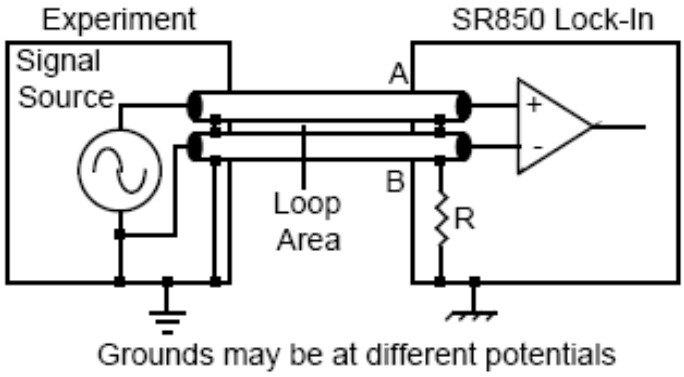

Figure 29: Differential voltage connection in the SR850 Lock in amplifier [58].

To achieve maximum sensitivity a circuit is designed to measure the difference current from the photodiodes. Figure 30 illustrates the circuit diagram. Sensitive measurements of the terahertz signals are made possible by using this configuration.

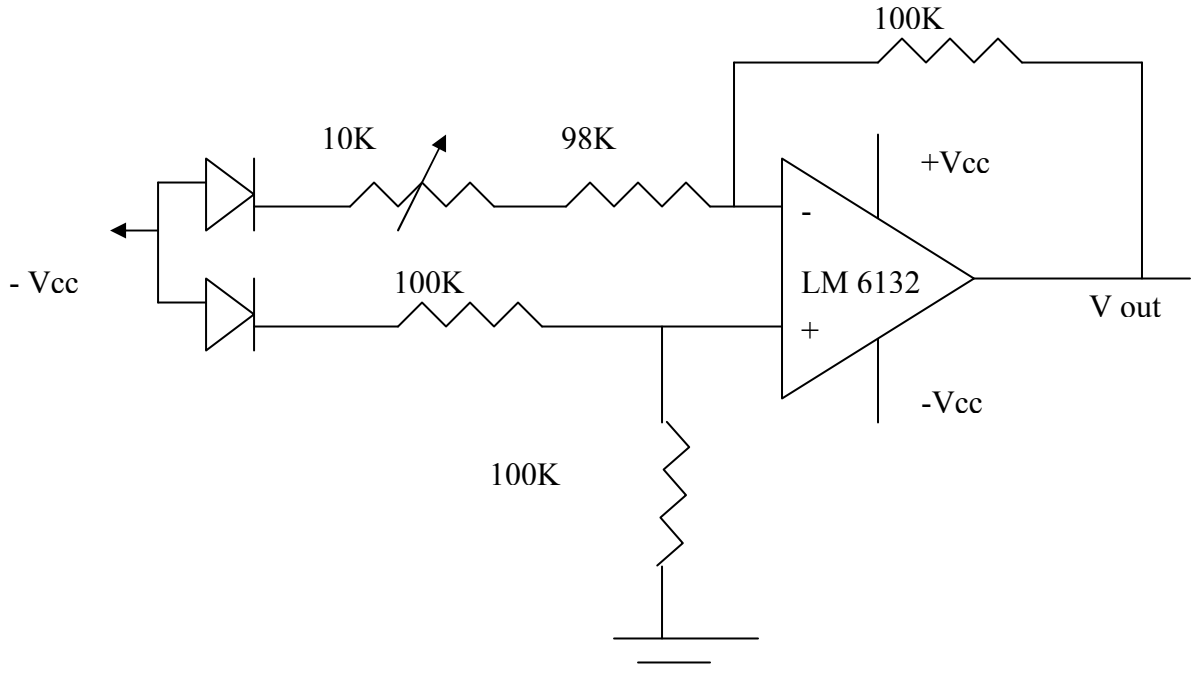

Figure 30: Illustration of balanced detection electronics

CHAPTER 4: RESULTS AND DATA ANALYSIS

4. 1 System implementation

We propose a solution for one of the major challenges in silicon semiconductor manufacturing which is the measurement of the absolute thickness of single side polished silicon wafers. We designed and implemented a terahertz time of flight detection instrument for characterizing semiconductor wafers in the transmission mode. Figure 31 shows the schematic of our technique. A detailed description of the technique and functions of individual components is given in chapter 3. The results presented in this chapter demonstrate the capabilities of our system. We discuss the calibration procedures and implementation method for optimal operation of the system.

4.2 Guidelines to calibration

The construction of the terahertz time domain metrology system requires precise alignment of the optical components. The experimental setup has a high degree of complexity because of the sensitivity required to detect the weak terahertz signal. The guidelines to calibrate the terahertz metrology instrument are divided into four parts.

- Laser setup
- Optical alignment
- Source setup
- Detector

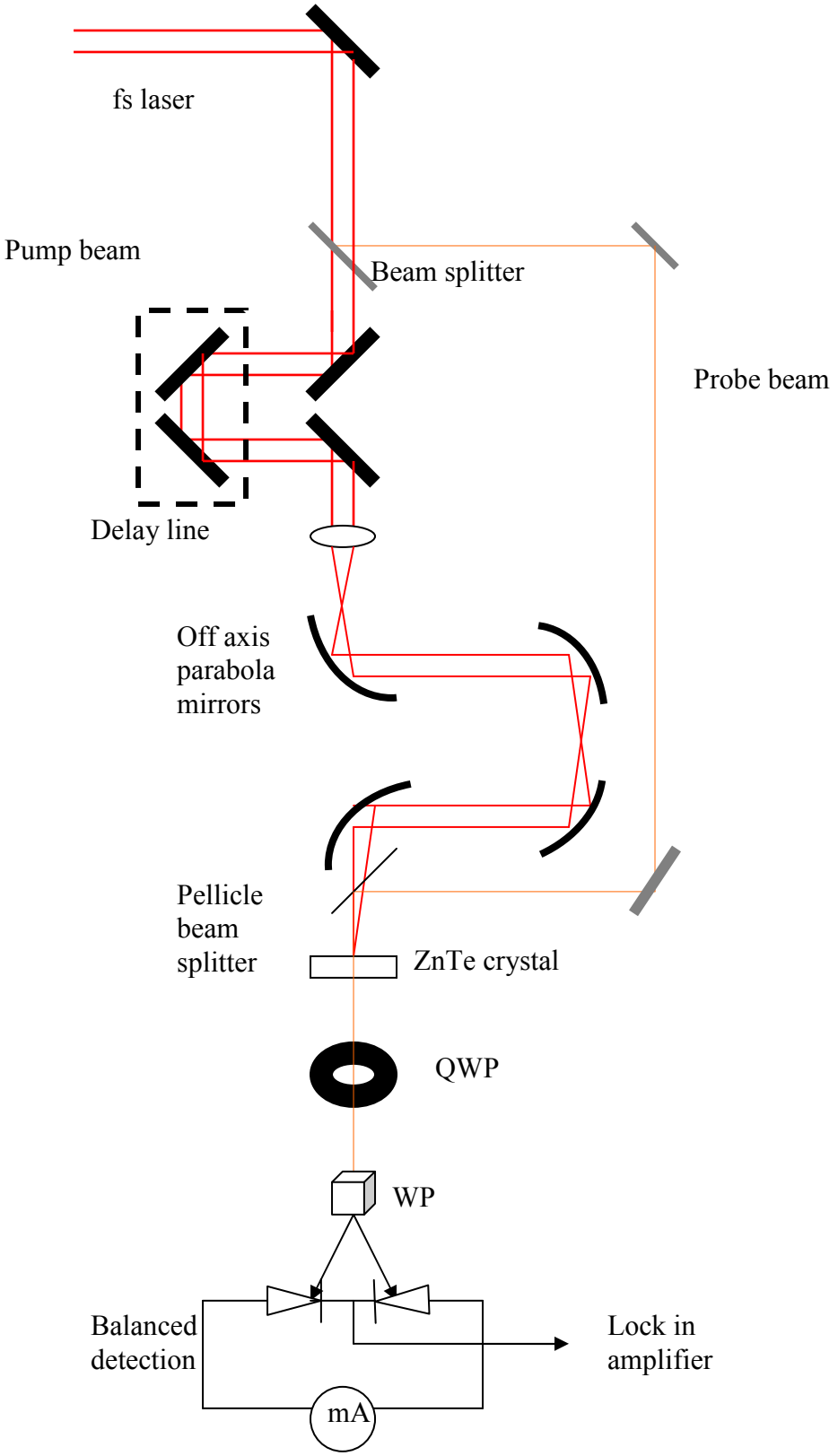

Figure 31: Schematic of terahertz metrology instrument

4.2.1 Laser

The terahertz system is powered by a Spectra Physics Tsunami Ti:Sapphire laser. The laser is pumped by a Spectra Physics Millenia V Nd-YAG laser. The chiller unit is turned on before activating the pump laser. We make sure the laser is at a suitable temperature and after a wait of around ten minutes the power is turned on the pump laser. The laser warms up and stabilizes the diode temperature. The pump laser has three modes on the main menu, power, current and RS232. For optimal usage and longevity of the laser, it is advised to operate it using the current mode. The current is gradually increased and at 40% current the Nd: YAG laser's green light is observed. The laser needs a warm up period of around half an hour. Mode locking should be ensured using an oscilloscope to view the femtosecond pulses. The femtosecond laser is nitrogen purged and the internal optics optimized for maximum efficiency. Once the laser mode locking is ensured, press the mode lock button on the laser control unit to lock the pulse. In order to turn the laser off, slowly lower the diode temperature in the pump laser. Once the current is down to 0 %, press the power button to turn the laser off. Turn off the chiller unit.

4.2.2 Optical alignment

Details of the components involving the optical setup are discussed in the preceding chapters. Alignment is one of the most critical aspects of a well calibrated terahertz system. The beam diameter of the femtosecond laser is 2.5 mm. To ensure detection of the terahertz pulse using our pump probe configuration, two conditions must be met:

- static overlap of pump and probe beams
- dynamic overlap of pump and probe beams

Since we are using a 90-10 beam splitter for splitting the incident femtosecond pulse into a pump probe configuration, the probe beam will be much weaker than the pump beam. Terahertz radiation is generated by the pump beam, then focused using off axis parabolic mirrors on a ZnTe crystal. The focused spot size is roughly 0.5 mm. In order to ensure overlap, the terahertz source is removed. The terahertz pulse and femtosecond optical pulses propagate collinearly and hence the path of the femtosecond laser beam can be considered to be the same for the terahertz pulse propagation through free space. The ZnTe detector crystal is mounted on an xyz translation stage. The crystal is replaced by a white screen to observe the overlap of the probe beam and the focused pump beam spot. Once overlap is observed, the white screen is replaced by the detector crystal.

For dynamic overlap, we need to ensure that the beam does not “walk off” during the motion of the delay line. To ensure dynamic overlap the optical delay line needs to be precisely aligned. This alignment is performed during the initial calibration and alignment of the optical components. We used the Veeco RTI 4100 interferometer to align the retro reflector mounted on the motorized stage. Figure 32 shows the alignment technique using the Veeco interferometer. The interference pattern between the reference beam from the transmission flat and the reflected beam from the retro reflector is observed as a fringe pattern by the interferometer. The tip and tilt of the retro reflector are adjusted to null the fringes, ensuring that the mirrors are oriented 90 degrees to each other. As a result, the movement of the motorized linear stage does not affect the orientation of the laser pulse during the scan.

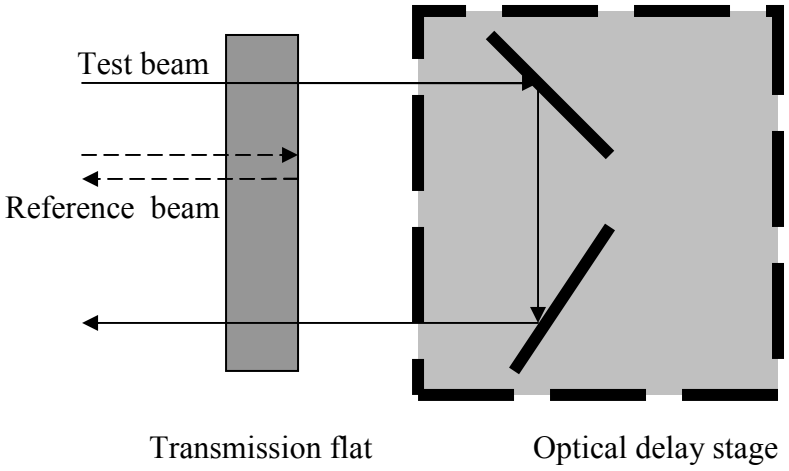

Figure 32: Alignment of delay stage retro reflector using a Veeco interferometer.

4.2.3 Source setup

As described in the previous chapters, the source used for terahertz detection is the photoconductive antenna. The antenna was purchased from Zomega Terahertz Corp. The configuration is a strip-line antenna. It consists of two metallic leads with a 150 μm gap deposited on a GaAs substrate. The laser is focused on the gap between the metal leads. The antenna is supplemented by a high voltage modulator also provided by Zomega terahertz corp. Figure 33 shows the high voltage modulator. The terahertz signal at the output of the lockin amplifier has an amplitude on the order of micro volts. The bias applied to the metallic leads is modulated with a function generator and this reference frequency is input to the lockin amplifier. The amplitude of the bias is adjusted on the high voltage modulator hardware interface. When the optical pulse is focused on the gap between the metal leads, the free charge carriers are accelerated under the action of the bias field. A bias of 70 to 150 V modulated at 10 kHz generates a strong terahertz signal. A labview program is provided by the antenna manufacturer to help in the

alignment of the antenna to the femtosecond source beam. The high voltage modulator signal is input to the computer through a USB port. As the bias voltage is increased on the hardware, the current signal is recorded on the labview program. The measured current indicates the presence of a generated terahertz electric field. Figure 34 shows the program control window. The antenna is positioned and adjusted in space so the femtosecond focus is coincident with the antenna and a maximum current signal is detected.

Figure 33: High voltage modulator for photoconductive antenna [59].

4.2.4 Detector setup

The static and dynamic overlap of the pump and probe beams on the ZnTe crystal is also critical. The polarization change of the probe beam is detectced using electro optic sampling. The orientation of the detector crystal needs to be rotated and a maximum detector signal is achieved. This is because the detected terahertz signal depends on the azimuthal angle of the detector crystal compared to the linear polarization state of the reference beam. The quarter wave plate is rotated to minimize the difference current

signal from the photodiodes. For a stable measurement, the difference current is on the order of 3 to 10 mV. This signal is input to the lock in amplifier. The reference signal from the function generator (that drives the antenna) is also input to the lockin amplifier . The lockin amplifies the component of the terahertz signal at the reference frequency. Figure 35 illustrates the measurement technique.

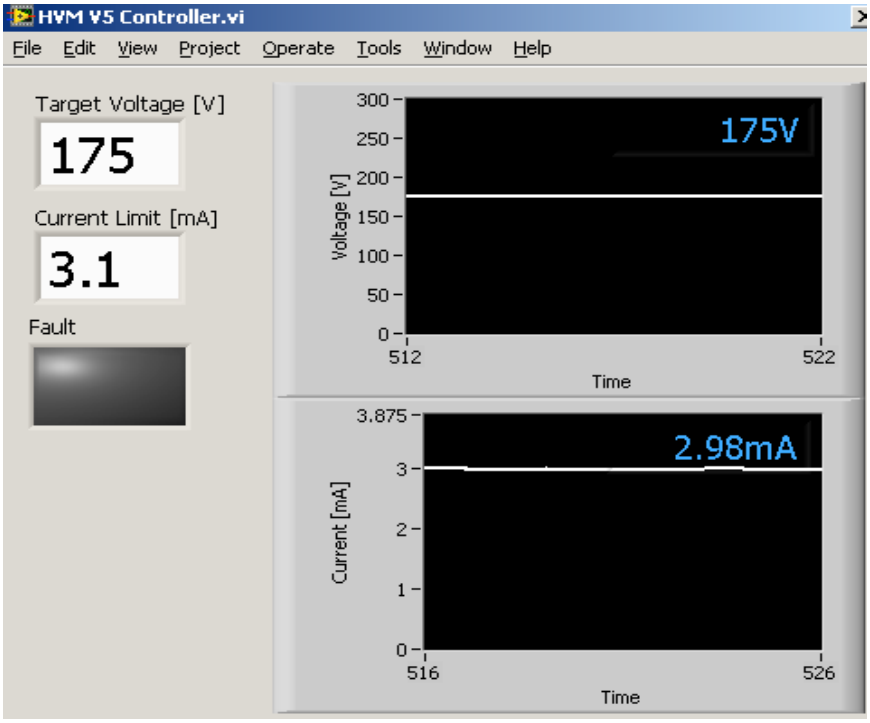

Figure 34: Labview alignment tool for photoconductive antenna [59].

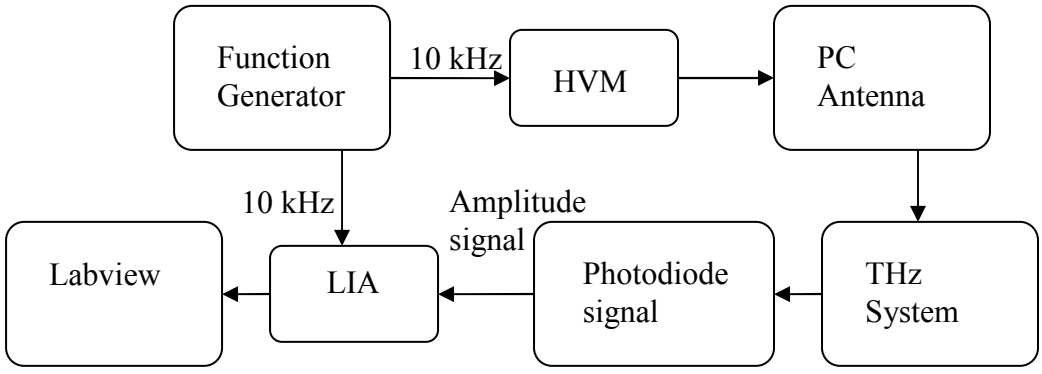

Figure 35: The function generator input to the high voltage modulator (HVM) causes the

THz repetition rate to be 10 kHz. The terahertz signal is extracted by referencing the lock in amplifier (LIA) with the same 10 kHz signal.

The time constant of the lock in amplifier is set to 30 ms and the sensitivity is set to 500 uV. We developed a labview program to control the terahertz system and this is shown in figure 36. The front panel sets the length of the scan and selects the parameters being measured.

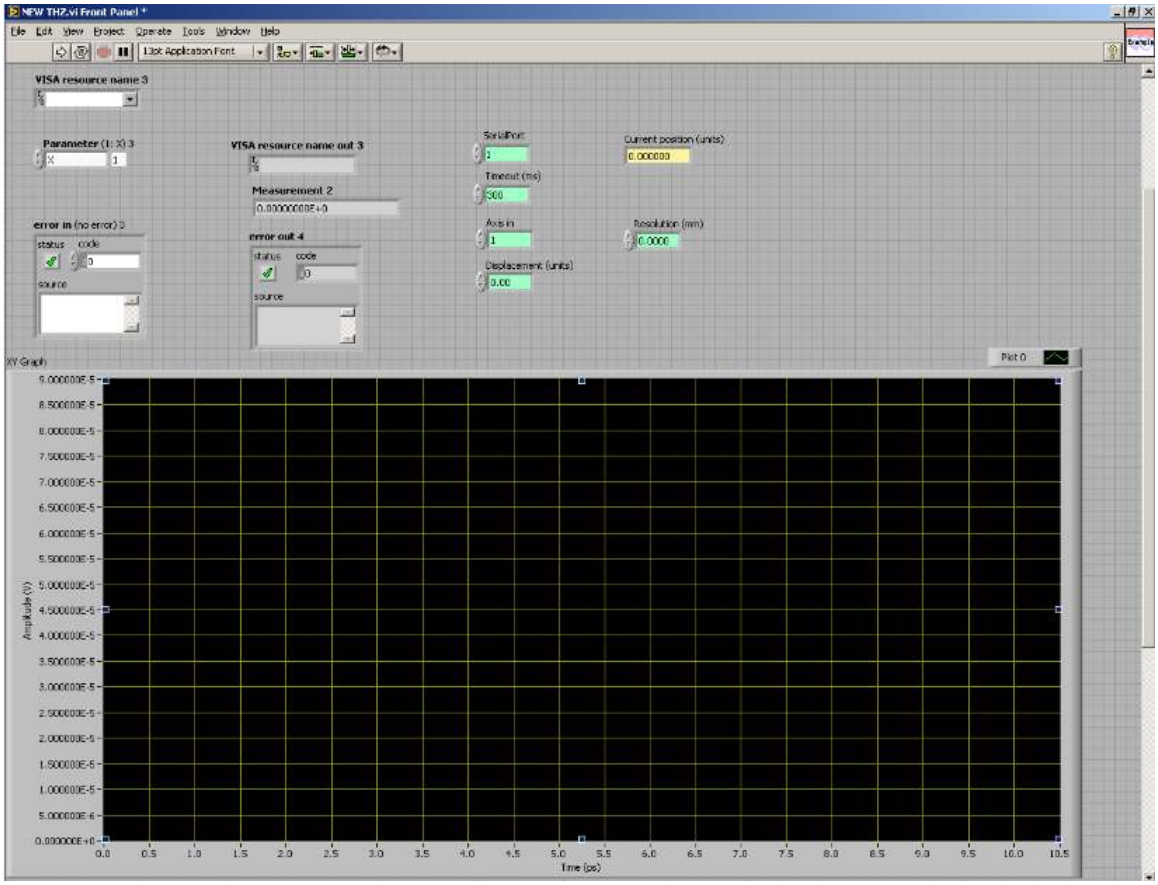

Figure 36: Front panel of terahertz system labview VI

4.3 Free space terahertz measurements

The terahertz signal measured in free space is shown in figure 37. The step size of the motor is set to 3 μm. The FWHM of the measured signal is calculated using MATLAB and found to be 0.32 ps. This value is close to the FWHM of a strip-line

antenna reported in the literature [7]. The spectral content is calculated by taking a Fourier transform of the signal. The spectrum associated with the spectral content of our measured terahertz beam is shown in figure 38.

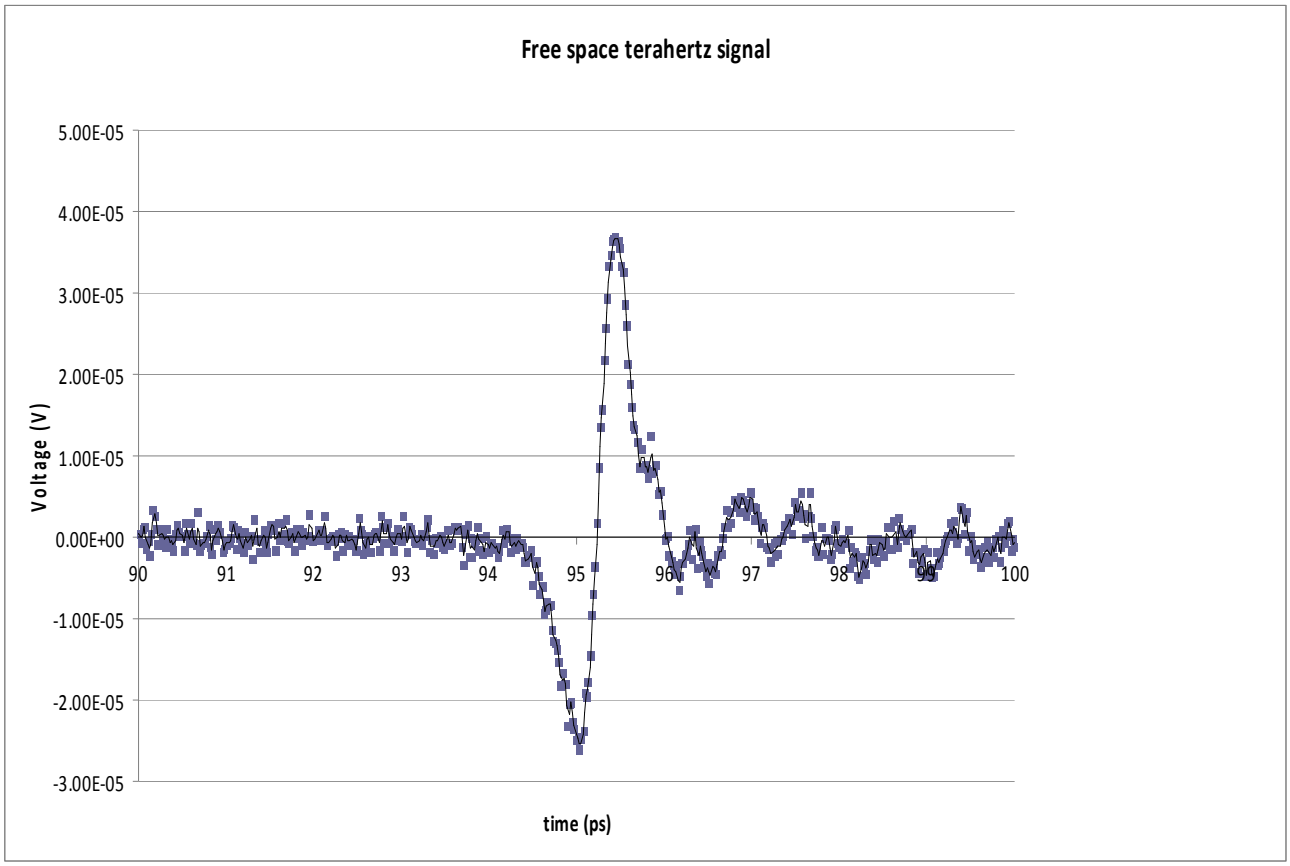

Figure 37: Free space terahertz waveform.

The motor is capable of moving a distance of 40 mm. The labview program that controls the motion of the motor is capable of real time resolution variations. For our experiments, the free space terahertz waveform was observed when the motor translation was 14 mm. As a result we scan at a higher speed till we reach 12 mm and then slow the motor to the minimum possible resolution of 3 μm. As a result we minimize the scan time and maximize sensitivity. The time for one scan is less than 5 minutes. The data is graphed in real time and also sent to a file for post processing.

4.4 Multiple reflections

Figure 39 shows an extended scan of the free space terahertz waveform. The scan is taken with a step size of 3 μm. We observe that the main pulse is accompanied with multiple echo pulses. These pulses are a result of internal reflection of the optical elements that comprise the terahertz system such as beam splitters etc. The echoes that appear after the main pulse are a result of internal reflections in the pump beam. There can be echo pulses before the main pulse as well which are a result of multiple reflections in the probe beam [32]. These reflections may be removed if required by post processing of the terahertz pulse.

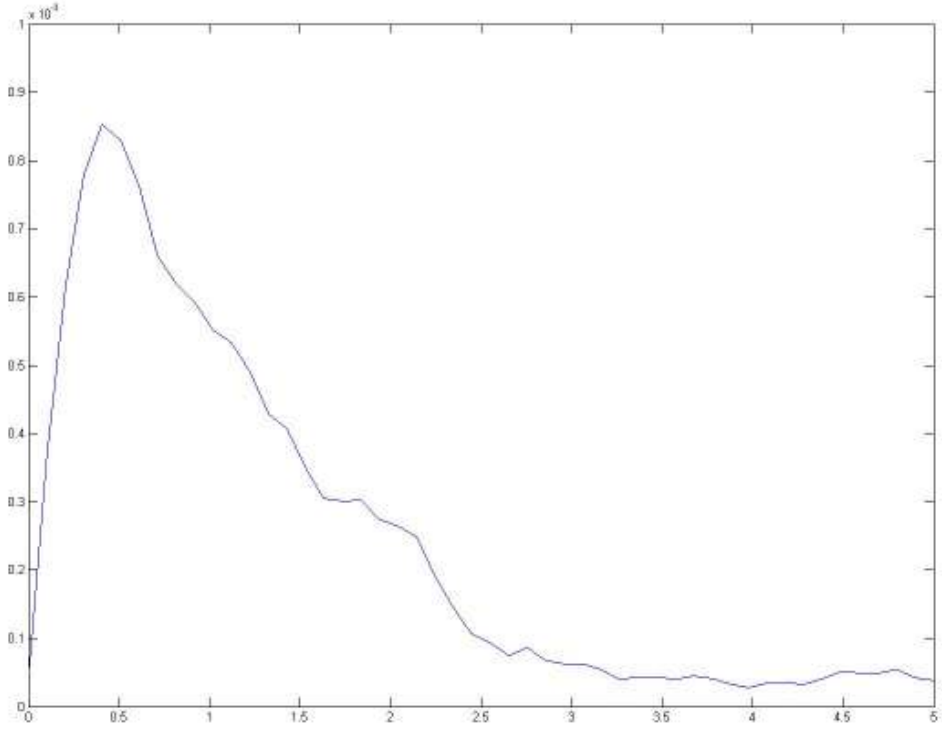

Figure 38: Spectral content of the terahertz waveform

4.5 Semiconductor metrology using terahertz radiation

In order to extract information about a material using terahertz radiation, a transmission measurement can be done where the terahertz pulse is propagates through the material. A comparison between the resultant pulse and a reference free space pulse in the time domain enables us to derive various quantitative conclusions about the material.

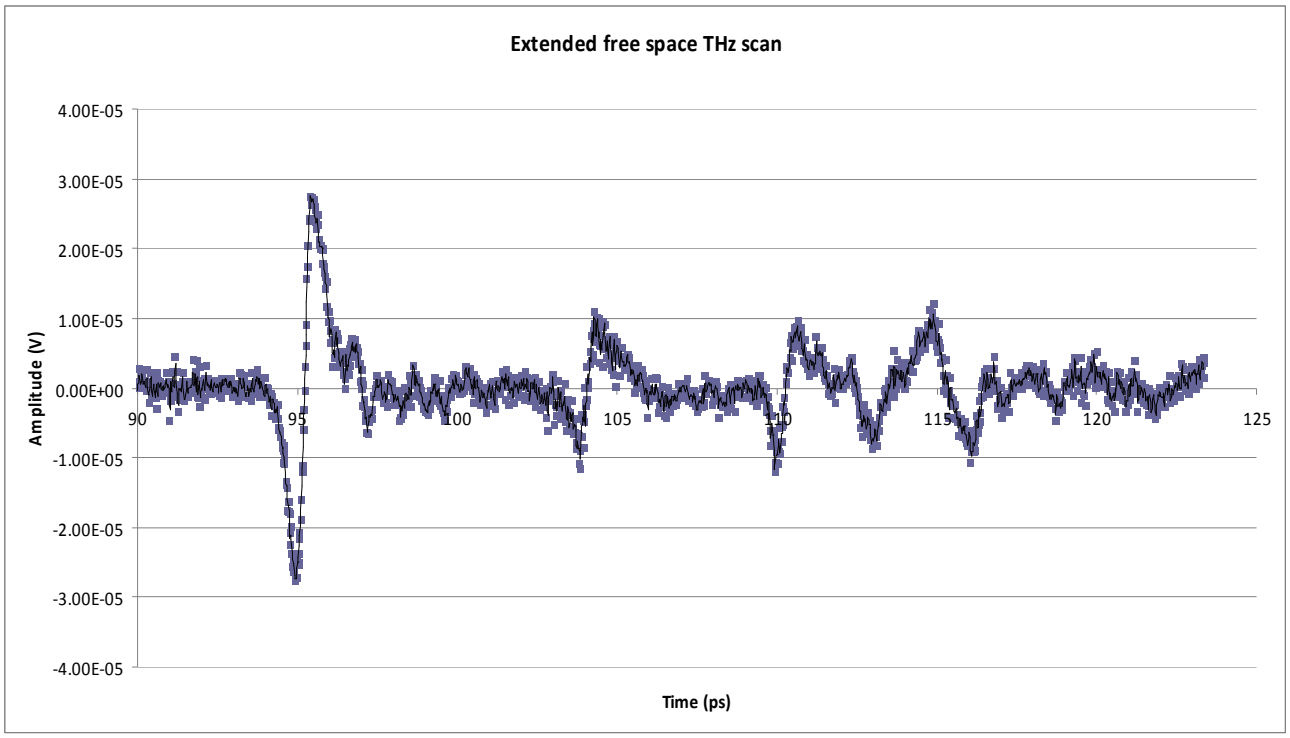

Figure 39: Extended free space terahertz scan.

Our terahertz metrology instrument is designed for measuring samples in the transmission mode. Figure 40 shows a measured waveform with a high resistivity silicon wafer as a sample. The spot size of the terahertz beam on the sample is estimated to be 0.5 mm. The resistivity of this silicon wafer is 1-20 ohm-cm.

4.5.1 Measurement capability and correlation

Static repeatability is defined as the measure of inherent variability of the measurement tool itself. It signifies the repeated measurements in which the part is not

removed from the tool between measurements. A static repeatability analysis is performed for the reference silicon wafer. The wafer is placed at the focus of the terahertz beam and the thickness is measured with 8 scans. The thickness can be calculated by knowing the refractive index and temporal displacement of the terahertz pulses using the following formula [60].

$$D = \frac{c_o \Delta T}{n_{THz} - 1}$$

Table 4 shows the static repeatability analysis of the reference terahertz wafer. The mean of the measurements is calculated to be 381.0 μm and a standard deviation of 3.0 μm. The sample was measured previously at the terahertz research labs at Rensselaer Polytechnic Institute (RPI) in Troy, New York. The terahertz research group at RPI is considered one of the leading research groups in terahertz research. Measurements of the sample were taken using two terahertz systems. The first system used is the Mini-Z commercial terahertz spectrometer [61]. Measurements are taken in reflection mode configuration and the thickness calculated. Figure 41 shows the measured waveform from the commercial terahertz system. The thickness on the commercial system is measured to be 379.3 μm. The second system used to measure the silicon wafer was the experimental setup using p-InAs semiconductor wafer as the source for the terahertz radiation. Figure 42 shows the waveform obtained by this system. The system measures the wafer in transmission mode. The yellow graph is the delayed waveform of the silicon reference wafer while the black graph shows the free space propagation of the terahertz waves. Measurements taken from the system are shown in table 5. The mean was calculated to be 371.0 μm and a standard deviation of 4.6 μm.

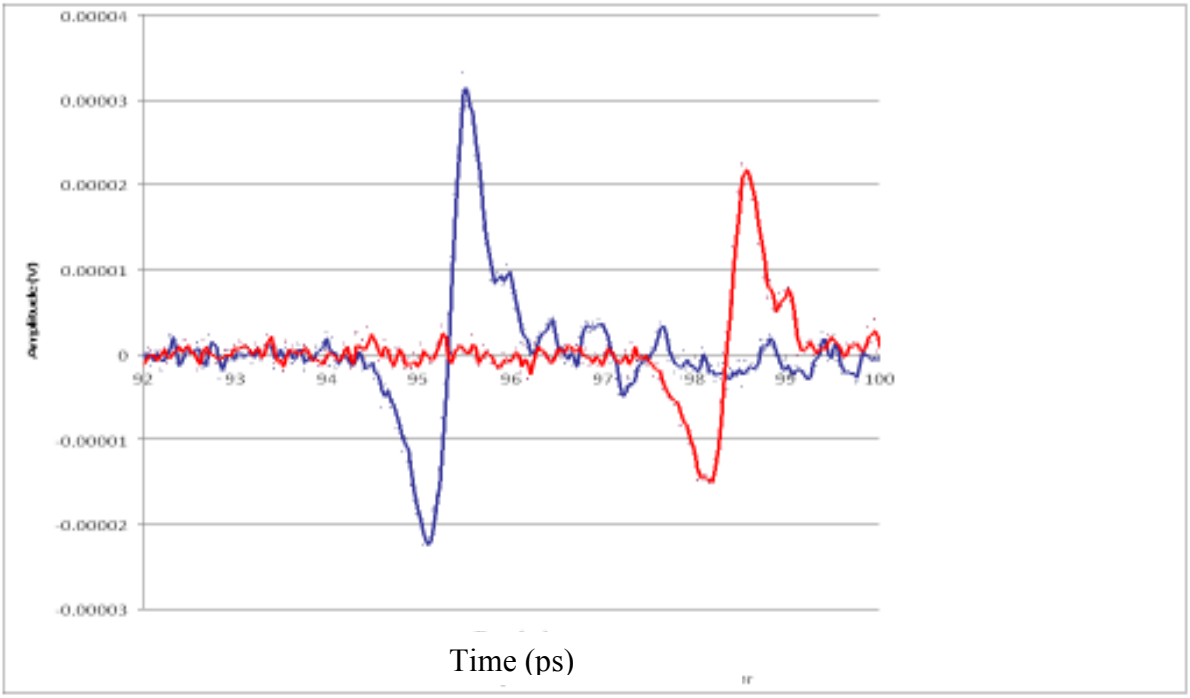

Figure 40: Temporal delay caused by a sample between freely propagating terahertz wave.

ΔT (ps)	**D (μm)**
3.0641	383.0
3.0661	383.6
3.0665	383.1
3.0627	382.8
3.0325	379.0
2.995	374.9
3.0331	379.1
3.0658	383.2

Table 4: Repeatability analysis of reference silicon wafer.

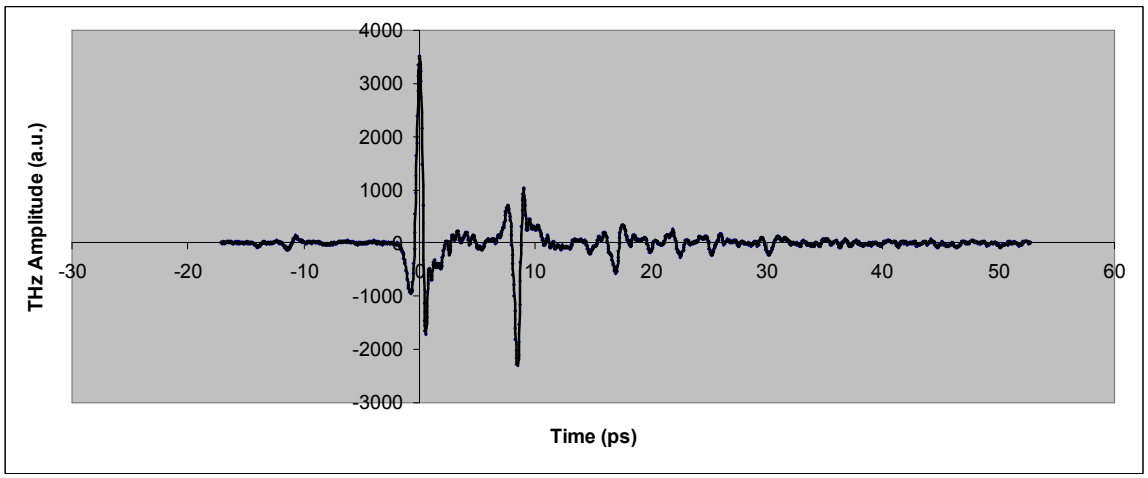

Figure 41: Measured transmission mode terahertz waveform from the mini-Z commercial terahertz system.

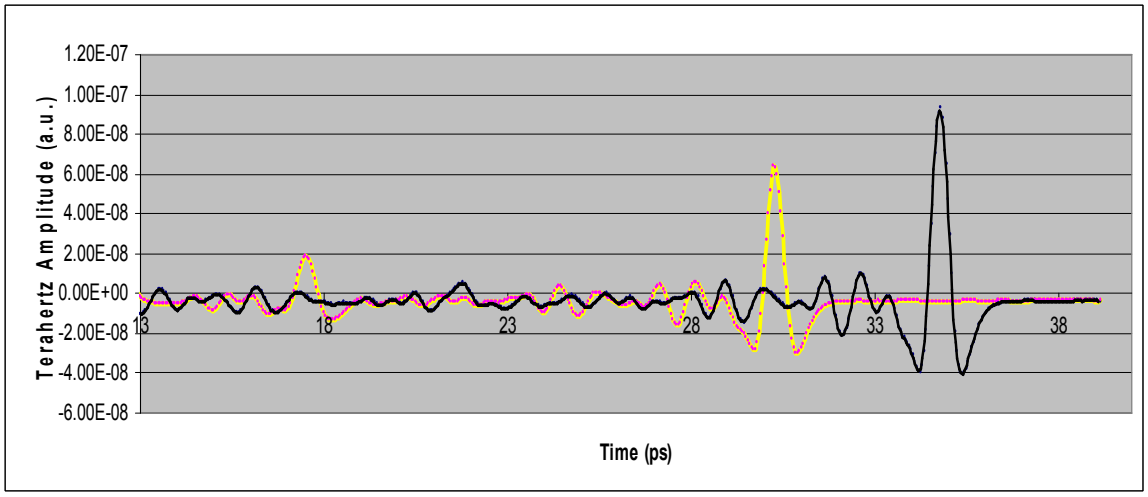

Figure 42: Transmission mode terahertz system with p-InAs wafer as source of terahertz radiation.

D (µm)
376.3
365.2

371.0
376.3
373.6

Table 5: Thickness measurements with p-InAs wafer source terahertz system.

4.5.2 Metrology of single side polished/etched wafers

Infrared transmission has been used in the semiconductor industry for measuring silicon crystals. Ellipsometry is employed to measure the thickness of films deposited on silicon [62]. *Parks et al* demonstrated the use of non-contact optical interferometry to measure the thickness, total thickness variation and bow of a silicon wafer. They used phase shifting interferometry at infrared frequencies and analyzed haidinger fringes to obtain thickness information of the wafer. The system is limited to measuring only double side polished silicon wafers. A rough back surface destroys the spatial coherence of the light enough to eliminate haidinger fringes [63]. *Schmitz et al.* describe the use of infrared interferometer developed at the National Institute of Standards and Technology (NIST) to measure the thickness variation in silicon wafers. The interferometer also makes use of haidinger fringes and as a result can only measure double-side polished silicon wafers [13]. Our terahertz metrology instrument demonstrates a fast measurement of single side polished or etched silicon wafer. All the wafer measurements reported are on single side polished silicon wafers. The results shown in the previous section indicate the stability and reliability of our measurement using our metrology tool.

4.5.3 Effect of doping on terahertz transmission

The tendency of AC electric fields to penetrate into conductors is referred to as the skin depth. If the conductor is much thicker then the skin depth at a certain frequency

then its behavior becomes a surface phenomenon rather then a volume phenomenon [64]. The skin depth is described to be a function of frequency and the momentum scattering time. The momentum scattering time expresses the loss of momentum of the electrons accelerated by the field

$$\delta = \frac{2}{\alpha}$$

At very low frequencies the attenuation coefficient α is given by

$$\alpha = (2\sigma_o \omega \mu_o)^{1/2}.$$

At higher frequencies such as infrared frequencies an effect called carrier absorption occurs and a different expression for attenuation is used [47]

$$\alpha = \frac{Ne^2}{m^* \varepsilon_o nc\tau\omega^2}$$

For a silicon semiconductor at room temperature and terahertz frequencies,

N is the carrier concentration and is on the order of 10^{18} electrons/cm^3 , or 10^{24} electrons/m^3 for a heavily doped wafer.. The variable *n* is the refractive index and is approximately 3.4 at 1 THz. The variable τ is the momentum scattering time and is approximately 10^{-13} s at room temperature. The effective mass values, m* = effective mass, are $m^*_{n\text{-type}} = 9.837 \times 10^{-31}$ kg and $m^*_{p\text{-type}} = 5.101 \times 10^{-31}$ kg.

The skin depth computations for doped silicon are shown in table 6

Doping	**Carrier concentration (carrier/m^3)**	**Frequency (THz)**	**Skin depth (mm)**
n-type	10^{24}	1	69.3

n-type	10^{24}	10	6937
p-type	10^{24}	1	35.9
Un-doped (p-type)	10^{19}	1	3569

Table 6: skin depth calculations for different parameters of silicon wafers.

Hence we see that undoped wafers are practically transparent to terahertz radiation while the penetration varies with the doping levels. Figure 43 shows the measurement of an N(100) P doped Silicon wafer doped at 1-20 ohm cm.

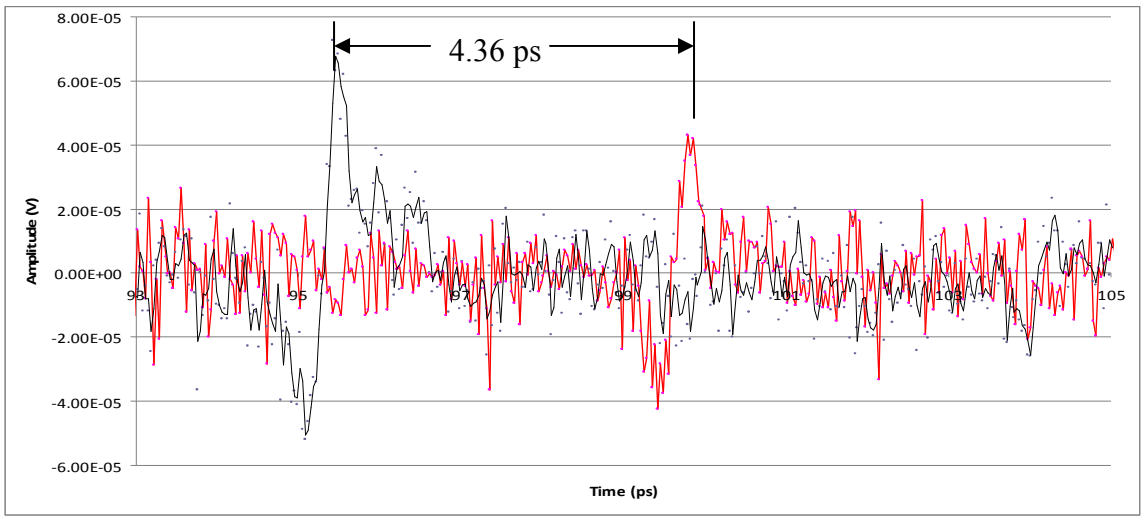

Figure 43: Measurement of N(100) p doped silicon wafer.

The thickness of the wafer is calculated to be 546 µm. The thickness of the wafer measured by a handheld micrometer 550 µm.

4.5.4 Thickness measurement of unknown material

When the refractive index of the material is unknown and the thickness can be estimated, the terahertz transmission measurement can be used to estimate the refractive index for the terahertz radiation.. Once the refractive index of the unknown material is calculated we may then use this calibrated value and measure other samples using that

refractive index. To demonstrate this, we choose packaging material as our unknown material. The formula for estimating the refractive index is;

$$n_{THz} = 1 + \frac{c_o}{D}\Delta t$$

Figure 44 shows the measurement waveform of packaging material. The refractive index at the terahertz frequency is measured to be 1.0122. This is intuitive since packaging material is mostly air hence explaining the proximity of the index to 1. Different samples of packaging material were measured and accurately correlated to actual thickness values.

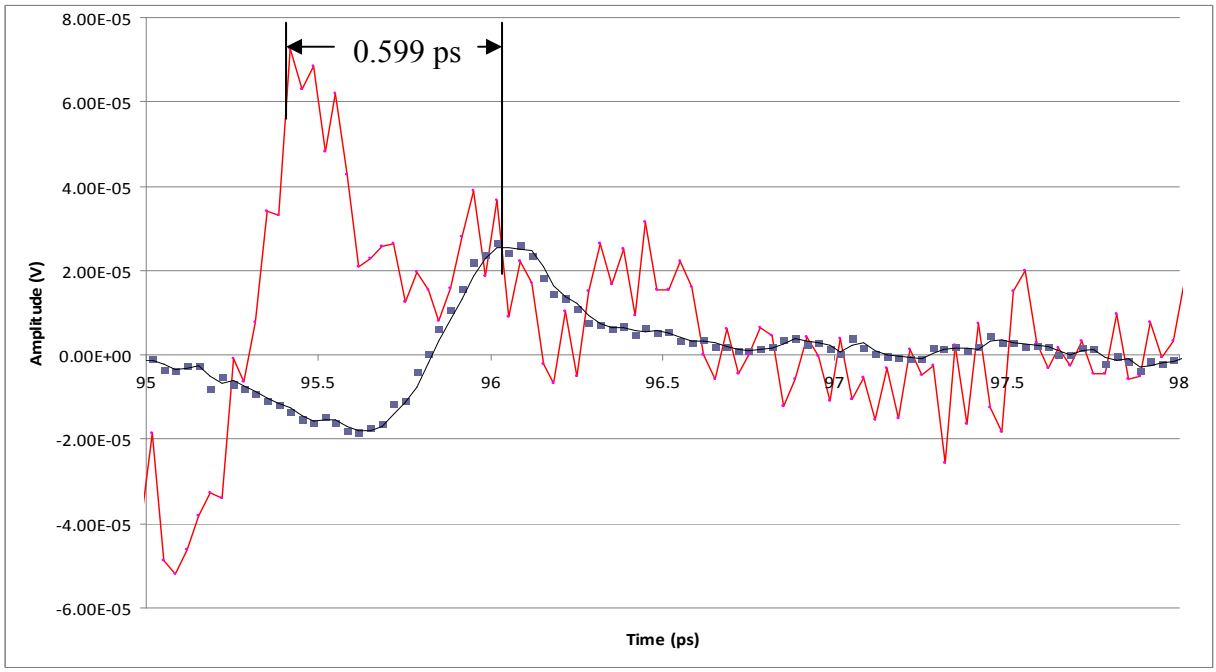

Figure 44: Measurement of unknown material.

CHAPTER 5: CONCLUSIONS AND FUTURE WORK

5. 1 Conclusions

The main results of this work are summarized as follows

- In this research various aspects of terahertz radiation such as generation, detection and propagation were studied. An extensive literature review has been performed on Terahertz source and detector technology, the leading research groups have been identified and an understanding of the potential applications and limitations of Terahertz radiation has been completed. The features of terahertz radiation such as its non-ionizing nature, low scattering, penetration into insulating materials, and unique spectroscopic signatures of many materials in this spectral region make it useful for many applications.
- One of the main sources for terahertz radiation is the photoconductive dipole antenna. It is made up of lithographically deposited metal leads on a semiconductor substrate. The incident femtosecond laser pulse accelerates charges which emits terahertz radiation. A nonlinear electro optic crystal can also be used as a source of terahertz radiation. When the non linear crystal is subjected to a high intensity pulse of sub-picosecond duration, it emits a pulse of terahertz radiation through a nonlinear optical process. In order to detect terahertz radiation, a photoconductive antenna can be used. The incident terahertz beam

and the femtosecond pulse induce a current that can be measured. Another method to detect terahertz radiation is free space electro optic sampling. The femtosecond and terahertz pulses are incident on the non linear crystal at the same instant creating a change in the polarization state which is measured by balanced detection optics.

- A reliable transmission mode time domain terahertz instrument was created which enables the measurements of a wide variety of specimens. The realization of our terahertz metrology tools opens the door to research and exploration into the applications of terahertz radiation in precision metrology
- The terahertz time domain metrology system was used to measure the thickness of silicon wafer of different types. A measurement capability and correlation analysis of our system was performed by characterizing the thickness of lightly doped single sided silicon wafers. This is a challenging measurement in a manufacturing environment and a terahertz approach represents a significant advance.
- The thickness and refractive index estimate were done on an unknown packaging material. Our experiments proved that the technique may be used to accurately measure the thickness of samples whose material properties are unknown beforehand.

5.2 Future work and projects

5.2.1 Development of reflection mode terahertz system

The terahertz metrology system implemented in this work is designed in the transmission mode configuration. Reflection mode terahertz enables us to measure

objects deposited on metallic material. The existing system can easily be modified to take measurements in the reflection mode by replacing the 90 degrees off axis parabolic mirrors that focus the terahertz on the test sample to 30 degree or 60 degree off axis parabolic mirrors. This would enable reflection mode terahertz imaging using our existing capabilities. Figure 45 shows the terahertz metrology system in the reflection mode.

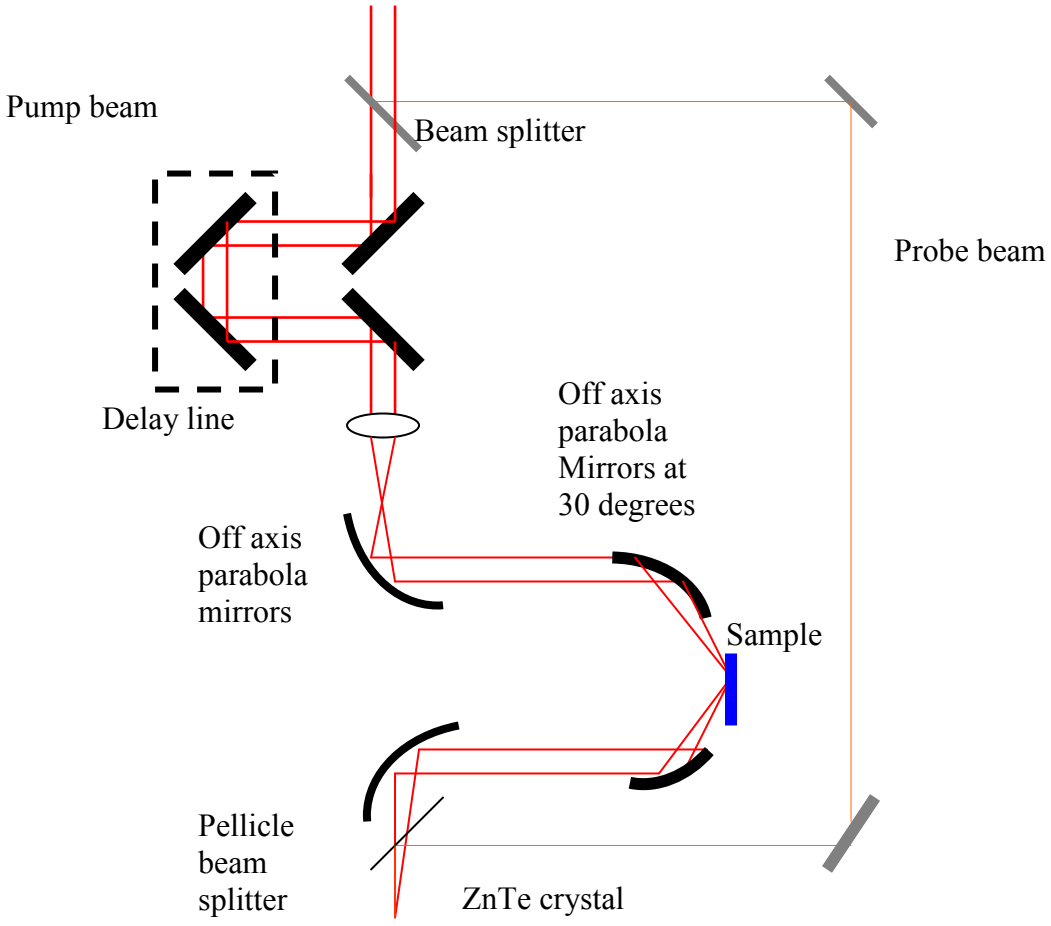

Figure 45: Terahertz metrology system in the reflection mode.

The system will be sensitive to the sample being measured since the reflection angle off the surface might destroy the overlap between probe and pump beam in the detector. This

challenge can be overcome by making a custom mount for sample placement which would ensure stability of the sample while dynamic measurements are made.

5.2.2 Further study of potential applications

This work may be extended to the measurement and analysis of material such as ceramics and composites. Also, biological samples can be measured using the terahertz metrology instrument. Terahertz radiation is strongly absorbed by water content of biological tissue. Terahertz spectroscopy enables us to study the spectral content of biological samples which can yield useful information. In the semiconductor industry the dryness of die after the manufacturing process is of specific concern. This may be a useful application to explore in the future.

5.2.3 Upgrading system components

The next generation terahertz metrology tool should have upgraded components. Some suggestions in this regard are as follows:

- A more sophisticated optical delay line would greatly enhance the dynamic range of the terahertz metrology system. The scan length of our current instrument is 40 mm. The motor is a Newport 850G linear actuator which is not in production at this time. The motor controller we used is the SMC 100 CC which does not provide a real time hardware interface and very limited options. The recommended motorized stage for the terahertz metrology instrument is the Thor labs NRT 100 linear translation stage. It provides a long travel of 100 mm and high precision with a minimum repeatable step size of 2 μm. Installing this device in our optical delay line will increase the scan length and accuracy of the results.

- Photoconductive antennas are used as a source of terahertz radiation in our system. The size of the gap between the metal electrodes determines the performance of the antennas. We use a strip line antenna configuration with a gap of 150 um. The performance of our terahertz system will be increased by using the antennas of smaller gap size which are available today. Gap sizes as low as 5 um are available. The recommended product is the E series photoconductive antenna provided by Zomega terahertz corporations. These antennas are fabricated with 50 μm, 100 μm, 150 μm and 200 μm gap sizes on a single chip and may be jumper selected.

REFERENCES

[1] X-C Zhang, “Terahertz wave imaging: horizons and hurdles”, Phys. Med. Biol. 47 (2002) 3667–3677

[2] Humphreys, K. Loughran, J.P. Gradziel, M. Lanigan, W. Ward, T. Murphy, J.A. O'Sullivan, C. “Medical applications of terahertz imaging: a review of current technology and potential applications in biomedical engineering”, Engineering in Medicine and Biology Society, IEMBS '04. 26th Annual International Conference of the IEEE, 2004

[3] Kodo Kawase, “Terahertz imaging- new steps toward real-life applications”, 12th International Conference on Terahertz Electronics, 2004

[4] Center for terahertz research, Rensselaer Polytechnic Institute, http://www.rpi.edu/terahertz/

[5] Pradarutti, B., Mattaus, G., Riehmann, S., Notni, G., Nolte, S., Tunnermann, A., “Advanced analysis concepts for terahertz time domain spectroscopy”, Optics Communications 279 (2007) 248–254

[6] Takeshi Yasui, Takashi Yasuda, Ken-ichi Sawanaka, and Tsutomu Araki, “Terahertz paintmeter for noncontact monitoring of thickness and drying progress in paint film”, Applied Optics, Vol. 44, Issue 32, pp. 6849-6856 (2005)

[7] Yun-Shik Lee, “Principles of Terahertz Science and Technology”, Springer, 2008

[8] Y.R. Shen, “Far infrared generation by optical mixing”, Prog. Quantum electron. 4, 207, 1976

[9] American society of non destructive testing. 2000. From http://www.asnt.org/

[10] Peter J. Shull, “Nondestructive evaluation: theory, techniques, and applications”, CRC press, 2002

[11] Štefan Kočiš, Zdenko Figura, “Ultrasonic measurements and technologies", Springer, 1996

[12] Malacara, D. “Optical shop testing”, Wiley-Interscience, 2007

[13] Tony L. Schmitz, Angela Davies, Chris J. Evans, “Silicon wafer thickness variation measurements using the National Institute of Standards and Technology infrared interferometer”, Opt. Eng. 42(8) 2281–2290 (August 2003)

[14] Amit Suratkar, “Absolute thickness metrology using wavelength scanning interferometry”, PhD dissertation, UNC Charlotte, 2009

[15] Xi-Cheng Zhang, “Introduction to THz Wave Photonics”, Springer, 2009

[16] Hertz, H., “Electric waves”, translated by D.E. Jones, Dover, New York, 1962.

[17] Auston, D.H., Cheung, K.P., Smith, P.R., “Picosecond photoconducting Hertzian dipoles”, Appl. Phys. Lett. 45 (3), 1984.

[18] Fattinger, Ch., Grischkowsky, D, “Terahertz sbeams”, Appl. Phys. Lett. 54(6), 1989

[19] Martin Van Exter, Fattinger, Ch., Grischkowsky, D, “Terahertz beams”, Appl. Phys. Lett. 55(4), 1989.

[20] Tani, M., Hirota., Que, Christopher., Tanaka, S., Hattori, Ryo., Yamaguchi, M., Nishizawa, Seizi., Hangayo, M., “Novel Terahertz Photoconductive antennas”, International journal of infrared and millimeter waves, Vol. 27, No.4, April 2006.

[21] Deibel, Jason., Mittleman, D., “FEM characterization of terahertz wave propagation on metal wire waveguides”, FEMLAB User conference presentation, Boston, MA, 2005.

[22] Reitten, Matthew T., “Spatially resolved terahertz propagation”, PhD Dissertation, Oklahoma state university, 2006.

[23] Chang, Q., Yang, D., Wang, L., “Broadband THz generation from photoconductive antenna”, Progress in electromagnetics research symposium, 2005.

[24] Namba, S., “Electro-optic effect of Zincblende”, Journal of Optical society of America, Volume 51, Number 1, 1960.

[25] Shen, Y.R., “Recent advances in non linear optics”, Rev. Mod. Phys. 48, 1-32.

[26] Auston, D.H., Cheung, K.P., “Coherent time domain far infra red spectroscopy”, J. Opt. Soc. Am. B, Vol. 2, No. 4, April 1985

[27] Zhang X.C., Ma X.F., “Determination of ratios between non linear optical coefficients by using sub picosecond optical rectification”, J. Opt. Soc. Am.B, Vol 10, No.7, 1993

[28] Zhang, X.C., Ma X.F., Rice, A., Jin, Y., “Terahertz optical rectification from <110> zinc blende crystals”, Appl. Phys. Lett. 64 (11), 1994

[29] Zhang, X.C., Wu Q., “Free space electro-optic sampling of terahertz beams”, Appl. Phys. Lett. 67(24), 1995

[30] R. W. Boyd, “Nonlinear Optics”, Academic press, Third edition, 2008.

[31] J. A. Valdmanis, G. A. Mourou, and C. W. Gabel, “Subpicosecond electrical sampling”, IEEE J.Quant. El. QE-19, 664 (1983)

[32] Khazan, Maxim., “Time domain terahertz spectroscopy and its application to the study of high T_c superconductor thin films”, PhD dissertation, University of Hamburg, 2002.

[33] Valk, N,. Wenckebach, T,. Planken, P., “Full mathematical description of electro optic detection in optically isotropic crystals”, J. Opt. Soc. Am. .B, Vol 21, No. 3, 2008.

[34] Rahanpura, K., Hargreaves, S., Lewis, R.A., “The generation of terahertz frequency radiation by optical rectification”, 33rd Annual Condensed Matter and Materials Meeting, 4-6 Feb. 2009.

[35] Jian, Z., “Terahertz photonic crystals”, PhD Dissertation, Rice University, 2006.

[36] Park, S, Melloch, M.R., Weiner, A,M,. “Comparison of terahertz waveforms measured by electo-optic sampling and photoconductive sampling”, App. Phys. Lett. Vol. 73, No. 22, 1998

[37] H. Zhong, A. Redo, Y. Chen, Xi-Cheng Zhang, “THz wave standoff detection of explosive materials”, Proc. of SPIE, Vol. 6212 62120L-2 (2006).

[38] H. Liu, H. Zhong, N. Karpowicz, Y. Chen, Xi-Cheng Zhang, “Terahertz spectroscopy and imaging for defense and security applications”, Proc. of the IEEE, Vol. 95, No.8, August 2007.

[39] J. Dickenson, T. Goyette, A. Gatesman, C. Joseph, Z. Root, R. Giles, J. Waldman, W. Nixon. “Terahertz imaging of subjects with concealed weapons”. Proc. of SPIE, Vol. 6212 62120Q-1, (2006)

[40]A. Nahata, J.T. Yardley, and T.F. Heinz, “Free-space electro-optic detection of continuous-wave terahertz radiation,” Appl. Phys. Lett. 75, 2524 (1999)**.**

[41] Q. Wu, T.D. Hewitt, Xi-Cheng Zhang, “Two-dimensional electro-optic imaging of THz beams”, Appl. Phys. Lett. 69 (8), 19 August 1996.

[42] Z. Jiang, X.G. Xu, Xi-Cheng Zhang, “Improvement of terahertz imaging with dynamic subtraction technique”, Applied optics. Vol. 39, No. 17, June 2000.

[43] B.B. Hu, M.C. Nuss, “Imaging with terahertz waves”, Optics letters. Vol. 20, No. 16, August 1995.

[44] J. Cunningham, C. Wood, A. Burnett, P.C. Upadhya, W.H. Fan, E.H. Linfield, A.G. Davies, "Terahertz time domain spectroscopy – present and future modalities", Microwave symposium, 2007, IEEE/MTT-S International

[45] T. Yasuda, T. Yasui, T. Araki, E. Abraham, "Real time two dimensional tomography of moving objects", Optics communication 267 (2006) 128-136.

[46] List-magnetik coating thickness meter, http://www.panametria.cz/PDF/NDT/EasyCheck.pdf

[47] Mark Fox, "Optical properties of materials", Oxford University press, 2006.

[48] Spectra-Physics. "Tsunami mode locked Ti: Sapphire laser. User's manual".

[49] Shu-Zee Lo, "Spectra-Physics Mode locked Ti: Sapphire laser", University of Maryland, 2007.

[50] P. Siegel, "Terahertz technology", IEEE transactions of microwave theory and techniques, Vol. 50, No.3, March 2002.

[51] D. Mittleman, R. Jacobson, M. Nuss, "T-Ray imaging", IEEE Journal of selected topics in quantum electronics, Vol. 2, No. 3, September 1996.

[52] C. Bruckner, et al., "Optimal arrangement of 90^{o} off-axis parabolic mirrors in THz setups", Opt. Int. J. Light Electron.Opt. (2008), doi:10.1016/j.ijleo.2008.05.024

[53] W. Chan, J. Deibel, D. Mittleman, "Imaging with terahertz radiation", IOP publishing, Rep. Prog. Phys. 70 (2007) 1325-1379.

[54] Newport corporation, "850G User manual".

[55] D. Turchinovich, J. Dijkhuis, "Performance of combined <100>-<110> ZnTe crystals in an amplified THz time domain spectrometer", Optics communications, 270 (2007) 96-99.

[56]http://www.ewh.ieee.org/tc/sensors/Newsletters/Number2/Center_for_THz_Research_at_Rensselaer.pdf

[57] T. Loffler, T. Hahn, M. Thomson, F. Jacob, H.G. Roskos. "Large-area electro-optic ZnTe terahertz emitters". Optics express (2005). Vol. 13, No. 14.

[58] Stanford research systems, "User manual. SR 850 Lock in Amplifier", 2007

[59] Zomega terahertz corp. "High voltage modulator user manual", www.zomega-terahertz.com

[60] F. Ellrich, M. Theuer, G. Torosyan, J. Jonuscheit and R. Beigang, “Thin film measurements with terahertz radiation”, 978-1-4244-2120-6, 2008

[61] Zomega terahertz corp. “Mini-Z user manual”, www.zomega-terahertz.com

[62] Alain C. Diebold, “Handbook of silicon semiconductor metrology”, Marcel Deker, 2001

[63] R.E. Parks, Shao, Lianzhen., Davies, Angela., Evans, C.J., “Haidinger interferometer for silicon wafer TTV measurement”, Proc. SPIE Vol 4344 (2001)

[64] Wheeler, Harold,. “Formulas for skin effect”, Proceedings of the I.R.E. 1942